Master's Degree
in
Energy and Nuclear Engineering

Fed-Batch Ex-Situ Biomethanation

Laboratory study and virtual modelling

Supervisor
Prof.ssa Mariachiara Zanetti

Co-supervisor
Eng. Giuseppe Campo

Candidate
Martino Ettore Ender

Academic Year 2024 - 2025

CONTENTS

ACKNOWLEDGEMENTS

Vorrei cogliere l'occasione per ringraziare tutte le persone che hanno reso possibile il mio percorso universitario e indimenticabili gli anni di studio al Politecnico.

Ringrazio per primi i miei tutor accademici, la Professoressa Mariachiara Zanetti per l'opportunità di partecipare all'interessante progetto su cui si è basata la mia tesi e l'Ing. Giuseppe Campo per la disponibilità, gli insegnamenti e i suggerimenti elargiti. Un grazie anche all'Ing. Alberto Cerutti per i consigli e per l'aiuto nello svolgimento delle attività in laboratorio.

Avrei davvero voluto condividere questo momento con mia nonna Caterina, che senza dubbio sarebbe stata ancora più felice ed emozionata di quanto lo sia io. Se sono la persona che sono il merito è solamente suo e penserò alle sue parole e ai suoi abbracci per tutto il resto della mia vita.

Ringrazio poi mia mamma Francesca, che mi supporta quotidianamente e mi aiuta a superare ostacoli che senza di lei sarebbero insormontabili, e mio papà Martin, che aiutandomi un migliaio di volte a sistemare la bici mi ha trasmesso la passione per la "razionalità ingegneristica". Fondamentale è anche il contributo di mio fratello Ettore e di mia sorella Caterina, che ogni giorno mi rallegrano condividendo con me le loro difficoltà e i loro successi.

Ringrazio anche la nonna Anna e lo scomparso nonno Martin, che nonostante la lontananza mi hanno sempre voluto bene e hanno cercato di starmi vicino in tutti i modi possibili.

Se durante gli anni dell'università ho vissuto esperienze incredibili e ho riso fino a stare male innumerevoli volte, è tutto merito dei miei amici.

Fra di loro spiccano Simo e Albi, con cui sono davvero grato di essere cresciuto e a cui mi rivolgerò sempre per sfuggire da periodi tristi o per condividere le esperienze più felici. Anche se la vita non ci permette più di vederci tutti i pomeriggi come ai tempi del liceo, il nostro rapporto rimane speciale come un tempo.

Andare in bici e fare sport sono diventati una parte fondamentale della mia vita, ma non sono sicuro sarebbe successo senza le splendide persone con cui mi alleno. Grazie a *mio fratello* Jack, a Pier e a Nano per i bei momenti e per i discorsi "trascendentali" che vengono fuori quando siamo insieme. Grazie anche a tutti i Broski-Loschi e le Turbolente che mi hanno fatto scoprire cosa significa viaggiare in tenda e andare in montagna: Matti, Cate, Ele, Eugi, Damians, Maya, Mati, Fra, Cori e tutti gli altri.

Seguire lezione non è sempre stato semplice, ma le ore passate in aula sono volate grazie a tutti i compagni di corso con cui le ho trascorse. Fra di loro ci tengo a ringraziare Lulla, con cui ho preparato gli ultimi esami e la tesi e che non solo ha dei bellissimi appunti ma è anche una bellissima persona, ed Enea, il mio ragazzo di campagna preferito con cui mi sono ritrovato in situazioni molto differenti da quelle tipiche delle aule del Poli. Grazie anche a Samu e Pol, che mi hanno distratto infinite volte e mi hanno impedito di laurearmi troppo presto.

Per ultimi ma non per importanza, ringrazio i miei compagni di liceo con cui non solo sono rimasto in contatto ma con cui passo ancora momenti straordinari. Grazie a Margo, che è sempre piena di iniziativa e disponibile in caso di bisogno. Grazie a Sokki, con cui per molti anni ho condiviso tutti i momenti più importanti e con cui ancora adesso mi trovo straordinariamente bene. Grazie a Richi, a Vero e a tutti gli altri.

ABSTRACT

To reduce carbon emissions, renewable energy sources are gradually becoming more and more common and new ways to exploit them are constantly researched. Among the different technologies, the concept of Power to Fuel allows the production of a fuel that is easy to use and to store, using only green electricity.

In this work a biokinetic and deterministic model of a fed-batch ex-situ biomethanation reactor is implemented and executed in the Matlab-Simulink environment, with the goal of assessing the impact that different variables have on the methane production and predict the results that can be obtained with a specific system. Before the construction of the model, a laboratory scale reactor was studied, and data were collected to then verify the correct working of the model.

In the Introduction chapter, the reasons behind the transition towards green energy sources are explained, along with the consequences of this transformation. The concept of Power to Fuel is described and the main advantages of the technology are reported. The processes of green hydrogen production and of carbon capture are analysed, being the fundamental bricks for all the Power to Fuel transformations. In the last part, the different synthetic fuels are compared, and the advantages of each one are reported.

The second chapter is related to the description of the biomethanation technologies. At first, the microorganisms that populate the system are introduced and classified, together with the different types of reactors and their main characteristics. As the most important parameter influencing the methane production rate, the gas-liquid mass transfer mechanism is described and possible ways to increase it are mentioned. At the end of the chapter the typical conditions present inside a biomethanation reactor are discussed.

The third chapter is about the experimental data collected from the laboratory scale reactor and starts with a comparison of the results obtained by different researchers with the ex-situ biomethanation process. Then the laboratory setup and the functioning of the reactor are described, before the analysis of the main data collected and their variations in time.

The fourth chapter describes the construction of the virtual model of the reactor and the analysis of the impact of the various parameters on the performance. Previous virtual models of biological reactors are discussed, in particular the Anaerobic Digestion Model N. 1, developed in 2002. Then the equations constituting the model are reported, along with the values chosen for the different parameters. To find the values of the gas-liquid mass transfer rate (kla) and microorganisms' concentration (X) parameters, the pressure curves simulated are matched with some of the experimental data collected. The pressure curves plotted with different values of these two parameters are then compared, together with the variations of the resulting Methane Evolution Rate and methane presence values. At last, the influence of the pressure inside the reactor is studied.

From the analysis it emerges that the gas-liquid mass transfer rate and the internal pressure have a major impact on the methane production and are the key to better performances, but it's clear that to reach high MER values an increase of the number of hydrogenotrophic methanogens is needed to fully exploit the higher kla and pressure. According to the simulations, increasing the kla of the laboratory reactor to the maximum reasonable values a MER of 8.1 $Nm^3/(Nm^3 days)$ can be reached with a methane presence of 96.3 %, while working at a high pressure (8 bar) the MER becomes 22.1 $Nm^3/(Nm^3 days)$ with 95% of CH_4. Considering the performance required, it's possible to use the virtual model to understand the characteristics needed from the reactor and to evaluate if the benefits obtained with a certain modification are satisfactory.

1. INTRODUCTION

1.1 Global warming and renewable energy systems

Up to the start of the 21st century, the world's energy production relied almost entirely on fossil fuels, like coal, oil and gas, but in the last decades a series of problems related to their usage emerged. First of all, they are finite resources: according to different research and simulations, considering the current consumption and the proven reserves, known oil reserves are for example going to run out in less than 50 years [1]. However, the main problem is not their remaining quantity, but the greenhouse gases released in the atmosphere by these fuels. By trapping the heat, these gases are responsible for global warming, the long-term heating of the Earth's surface.

During recent years, this issue has become vital, and countries are trying to set adequate policies and goals in order to limit the increase of the global temperature. In 2019 the Green Deal was introduced by the European Commission: the stated goal is to achieve climate neutrality by the year 2050, to keep the rise of the global temperature below 1.5° C. This is called the Net Zero Emissions (NZE) scenario, and it is one of the most optimistic programs for the CO_2 emissions' reduction.

In Figure 1 the maximum CO_2 emissions requested by the different plans can be seen with the related temperature increase expected.

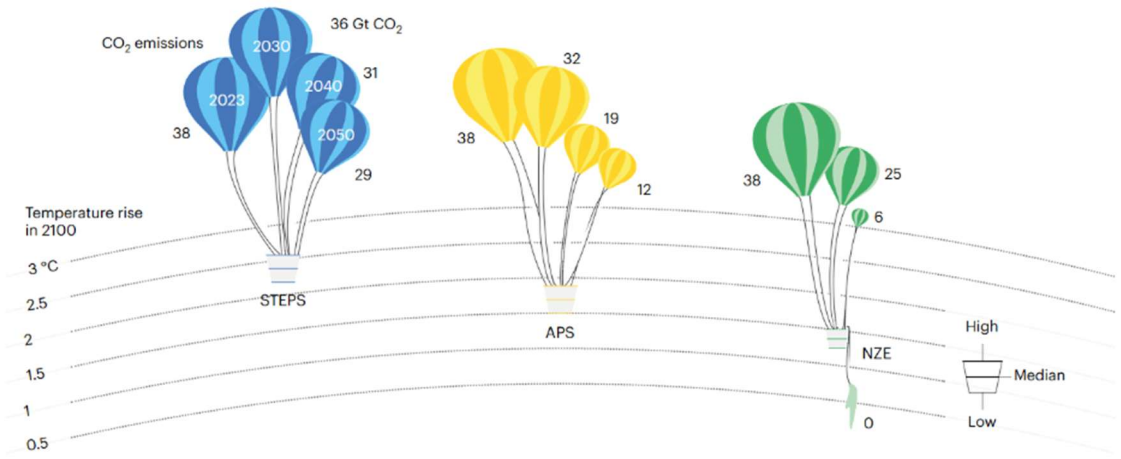

Figure 1 - Necessary CO_2 emissions' limits according to different plans [2]

These scenarios rely heavily on renewable energy systems (RES). The name renewable comes from the fact that they are replenishable sources that reform at a higher rate than they are consumed. Some examples are solar energy, wind power, hydropower and biofuels. In the last decades RES have rapidly developed, and they now occupy a key role in the majority of the energy sectors.

In Figure 2 the current energy mixes of the entire world and of Europe can be observed: 14.4 % of the world's total energy supply is produced by RES, while for Europe this value becomes 18.7 %. The share increases if it is referred only to electricity production, reaching a value of 38.2 % in the case of Europe.

To follow the global energy policies, the share of energy produced by renewable must consistently increase: Figure 3 shows the expected trend according to the STEPS, APS and NZE plans. According to the Net Zero pathway, by 2050 almost 90% of the electricity production will rely on RES, with solar energy and wind energy accounting for 70% of it [3].

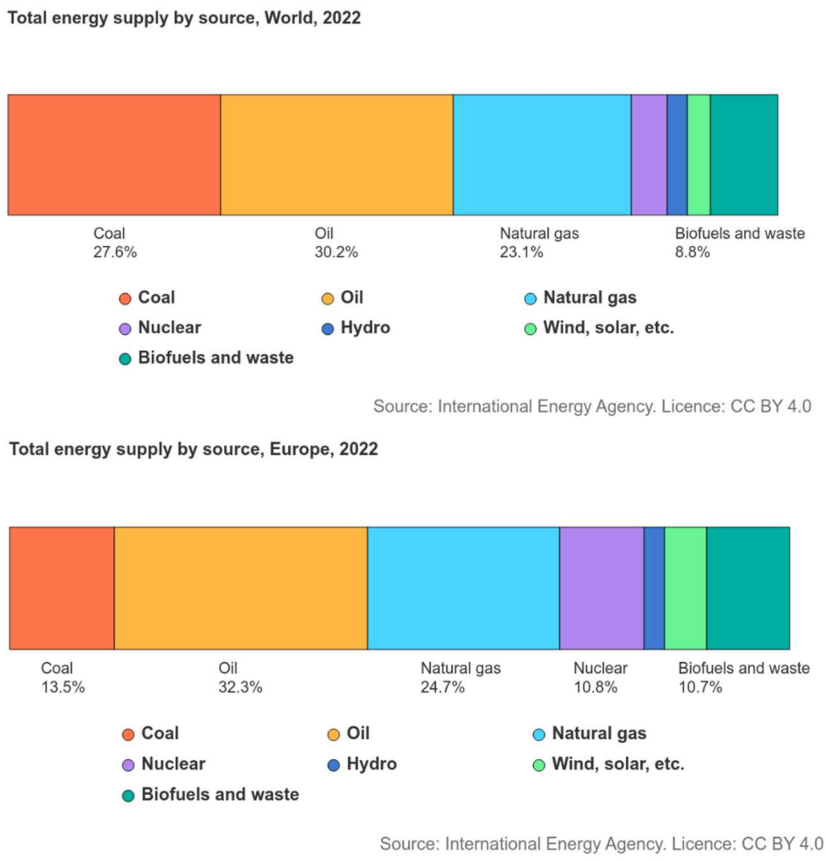

Figure 2 - Total energy supply by source [4]

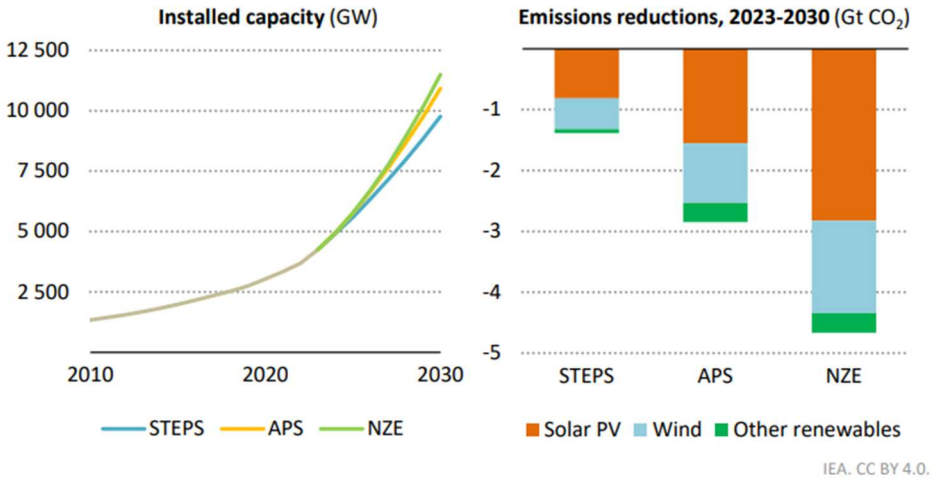

Figure 3 - Expected trends of installed capacity according to the different plans [2]

1.2 The concept of Power-to-Fuel (P2F)

The main disadvantage of the majority of RES is the impossibility to schedule the production according to the consumption and to know the exact amount of energy that will be produced at a certain time in the future. Even though general values like the annual capacity factor can be calculated with good approximation, the solar irradiance or the wind speed at a precise day and time can assume a relatively wide range of values. Nowadays this problem is not so crucial, because RES only cover a minor share of the total energy production and the fluctuations in renewable generation can be balanced by a correspondent variation in the production with fossil fuels. However, it's not always possible and it already happens that a certain amount of energy surplus has to be "wasted": the transmission operator has to pay the producer for not using the energy that should have been needed. For example, in China, an average of 7% of the total wind energy produced during 2018 had to be curtailed, with higher values in some of the regions. In 2017 in Ontario, Canada, around 25 % of variable renewable generation suffered the same fate and for almost a third of the year wholesale market prices were zero or negative [5]. In the future the share of energy produced by RES will rapidly increase and the fossil fuel powered system will not be big enough to balance the production.

In the case of standalone hybrid renewable energy systems, the surplus of produced energy is even more of an issue, as it can't be redirected using the grid and a high capacity factor is necessary to guarantee the availability of electricity. In these situations, many recent technologies become economically convenient, even though they still are not an optimal solution in grid-connected regions.

To solve this problem the power generated in excess has to be stored and used when the demand surpasses the production. A good solution is for example pumped storage hydropower, but it can't be implemented everywhere. Electricity can be also stored inside batteries: they have a good round trip efficiency (>90%) and can be rapidly charged or discharged, but the problem is that they are very expensive and need precious resources to be built. Other possibilities are compressed air and gravity storage, that cover a small role in current systems.

An emerging solution is the concept of Power to Fuel: the electrical energy is converted into chemical energy during the production of synthetic fuels. They can be used as a replacement for fossil fuels and similar to them they can be easily stored for long periods and transported. The most important ones are hydrogen, methane, methanol, dimethyl ether (DME) and ammonia. When the fuel is in gas form the process is called Power-to-Gas (P2G), while when the fuel is in liquid form the process is called Power-to-Liquid (P2L). In the image below different energy storage systems are compared. It can be seen that hydrogen and Synthetic Natural Gas are some of the most effective performing techniques.

The European Union believes that they will play a key role in the decarbonization of the transport sector and that they will also decrease the dependence on fossil fuels' import from foreign countries, which can lead to complex situations as it happened in the recent gas crisis related to the Russia-Ukraine conflict.

For this reasons Renewable Fuels of Non-Biological Origin (RFNBOs) are already taken into consideration in the Renewable Energy Directive II (RED II) [6] of 2009, revisited in 2018, and they are officially declared as a form of renewable energy regardless of the way in which they are used. In the subsequent Renewable Energy Directory III (RED III) [7], targets

are set for their utilization and by 2030 they should account for at least 1 % of the total energy supplied to the transport sector, exploiting at least 42 % of the hydrogen produced for energy applications by 2030 and 60 % by 2050.

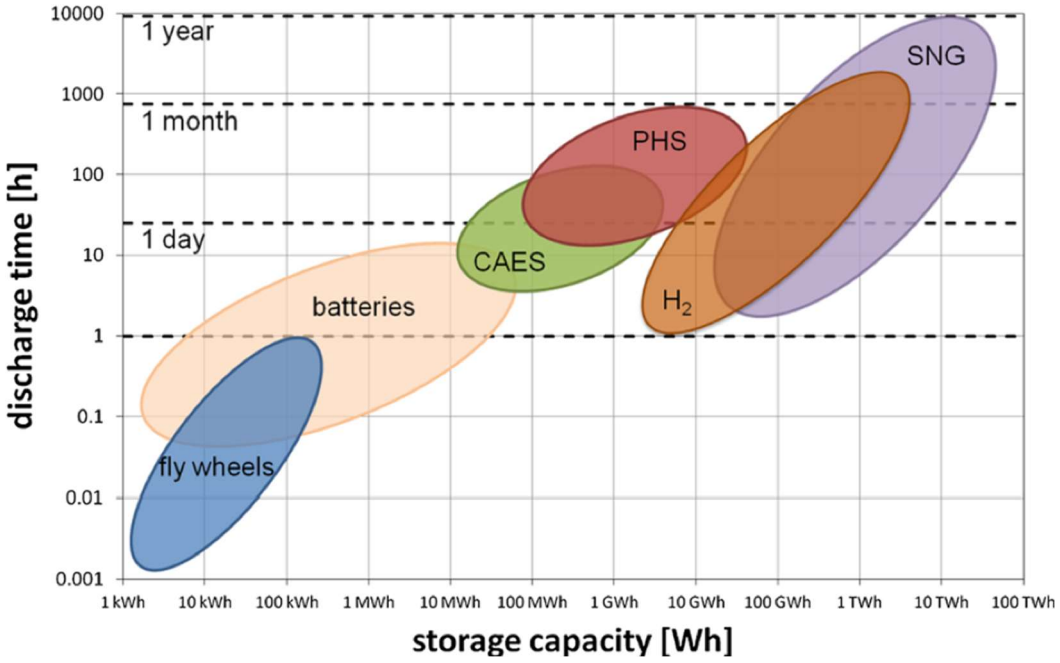

Figure 4 - Comparison between the different energy storage systems [8]

1.3 Hydrogen

Hydrogen electrolysis is the fundamental process behind the production of all green synthetic fuels, along with the recovery of carbon from biomass and carbon capture technologies. As it can be observed in Figure 5, nowadays H_2 is almost entirely produced starting from fossil fuels, mainly natural gas and coal. These processes are now way cheaper and easier to manage than green electrolysis.

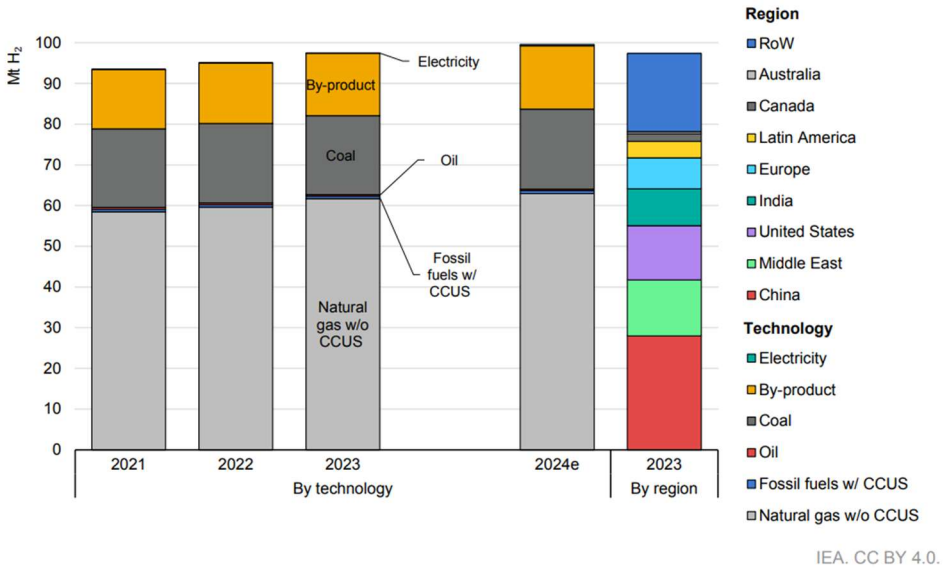

Figure 5 - Current methods for Hydrogen production [9]

This scenario is however destined to change, as an effect of the environmental policies discussed before: the constant development and research in RES will make the cost of green electricity lower and, considering also the economic penalties related to emissions, the price of green H_2 will soon be competitive with the one of the H_2 produced with fossil fuels. In figure 6 the diagram shows the expected cost of green H_2 production in 2030 in different world's regions, considering the already announced projects.

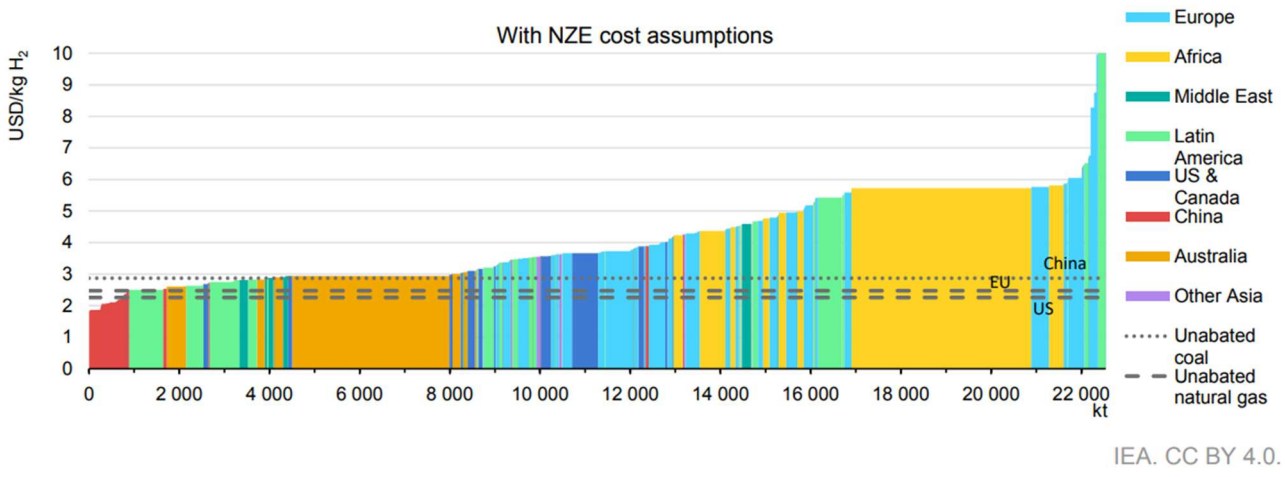

Figure 6 - Expected cost of green H_2 production in different countries in 2030 [9]

Hydrogen electrolysis is based on the following reaction, which is a non-spontaneous reaction ($\Delta G > 0$) and needs the electrical energy to happen:

$$2H_2O(l) \rightarrow 2H_2(g) + O_2(g)$$

During the electrolysis process, the electrical energy absorbed is exploited inside an electrochemical cell, where at the negatively charged cathode the hydrogen is reduced while at the positively charged anode the oxygen is oxidized. The main technologies used are alkaline electrolysis (AEL), polymer electrolyte membrane (PEM) and solid oxide electrolysis (SOEC) [10].

Alkaline electrolysis is most developed and the cheapest technology between the three. An aqueous solution with NaOH or KOH is used as an electrolyte to transfer the OH^- ions. The process can happen at atmospheric pressure or at elevated pressure. At atmospheric pressure the efficiency is higher but, if the hydrogen is subsequently pressurized, the overall energy used is lower in the case of the pressurized electrolysis. One of the drawbacks is the fact that the electrolytes used are highly corrosive and make the maintenance costs high.

PEM electrolyzers are a more recent technology, based on a solid polymer membrane which permits high proton conductivity with low gas crossover. At the sides of the membrane there are the electrodes, made with a catalyst material, usually platinum, to promote the reaction. Gas diffusion layers are situated at the other sides of the electrodes, to ensure the presence of the necessary number of reactants for the reaction to happen. The ionic conduction of the protons is much better than the one of the OH^- ions, ensuring higher currents. The main advantages of this technology are the higher flexibility, needed to efficiently exploit the electricity from renewable sources, and the higher purity of the H_2

produced. A negative aspect is that, because of the cost of the catalysts, the process is more expensive than the AEL electrolysis.

SOEC electrolyzers are even more recent than the PEM ones and are still at a laboratory stage. The electrolyte is made of ceramic material, usually yttria-stabilized zirconia, and is highly conductive for oxygen ions. The temperature is kept between 700 and 1000 °C, to decrease the equilibrium cell voltage and reach high efficiency values. Drawbacks of the high temperature utilised are the material degradation and the limited long-term stability. Reaching top level efficiency, SOEC technology is the most expensive between the ones discussed above.

In the image below, the three main technologies of electrolyzers are compared, along with the chemical reactions happening at the anode and at the cathode of the cells.

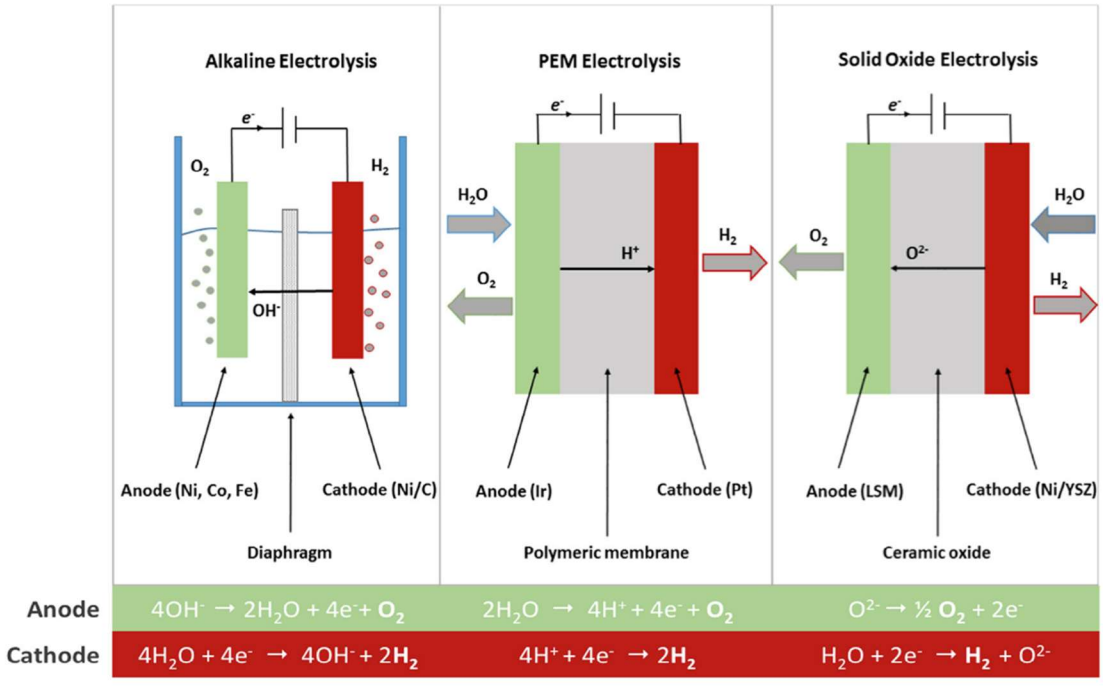

Figure 7 - Comparison between Alkaline, PEM and Solid Oxide electrolysis

1.4 Carbon capture

For the production of synthetic fuels, a carbon source like CO_2 is needed. Carbon dioxide is mainly obtained from separation techniques applied on the gases produced during industrial processes and from biomass decomposition. In general, the larger the presence of CO_2 is in the gas mixture, the easier and more efficient it is to remove it. Nowadays an often discussed source of carbon dioxide is biogas, because the CO_2 concentration in it can reach 50% and the removing of trace components like siloxanes and H_2S is relatively simple. Biogas plants are a relatively small source, but Power to Fuel processes don't need big quantities of carbon and if all the CO_2 removed from a power plant were to be exploited, the electrolyzers for the hydrogen production would need to be too huge and expensive [11]. In the diagram below, the relation between the minimum work for the capture and the CO_2 molar concentration is showed.

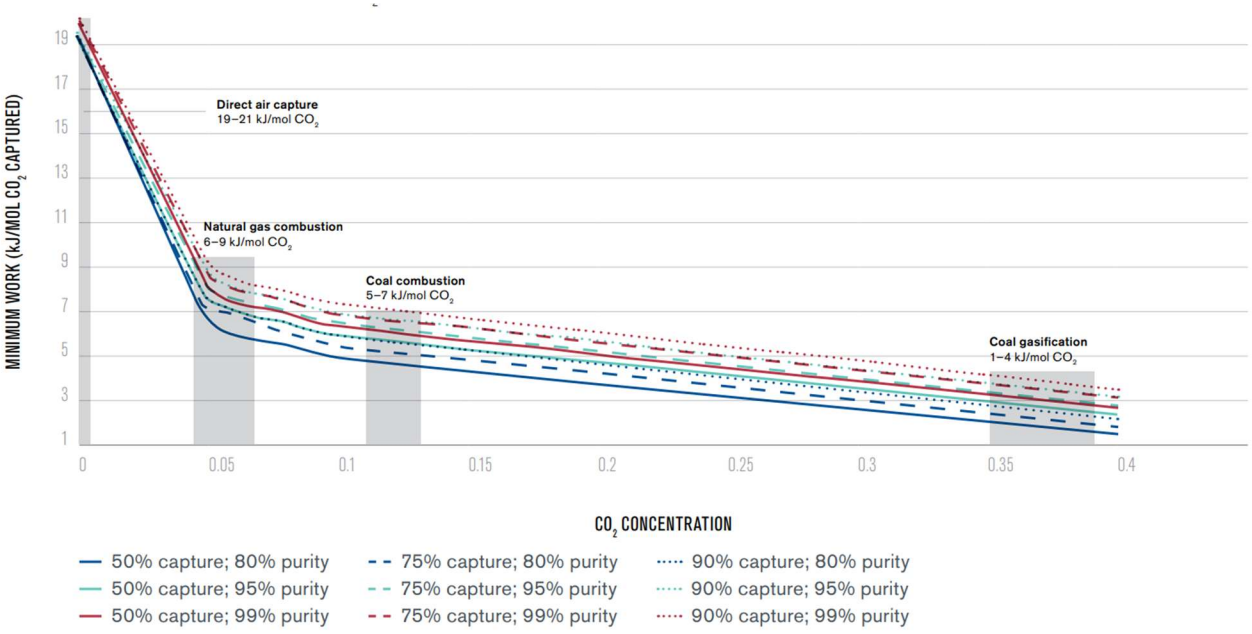

Figure 8 - Relation between the minimum work for the capture and the CO_2 molar concentrations at the inlet and at the outlet [12]

The main systems used for this process are post-combustion carbon capture, pre-combustion carbon capture and oxyfuel combustion [13].

- **Post-combustion**: the CO_2 is separated from the flue gases exiting the combustion chamber. The main advantage is that it can be easily retrofitted on existing plants. Often the separation is made with chemical solvents which then require high energy to be regenerated.
- **Pre-combustion**: before the combustion fuels are transformed into a mixture of H_2 and CO_2, easy to separate, and only the hydrogen part is burned. A disadvantage is that the gasification systems are expensive and complex.
- **Oxyfuel combustion**: the oxygen is separated from the air and enters alone the combustion chamber, producing flue gases made only of CO_2 and steam, easy to separate. The downside is the big amount of energy required for the oxygen production.

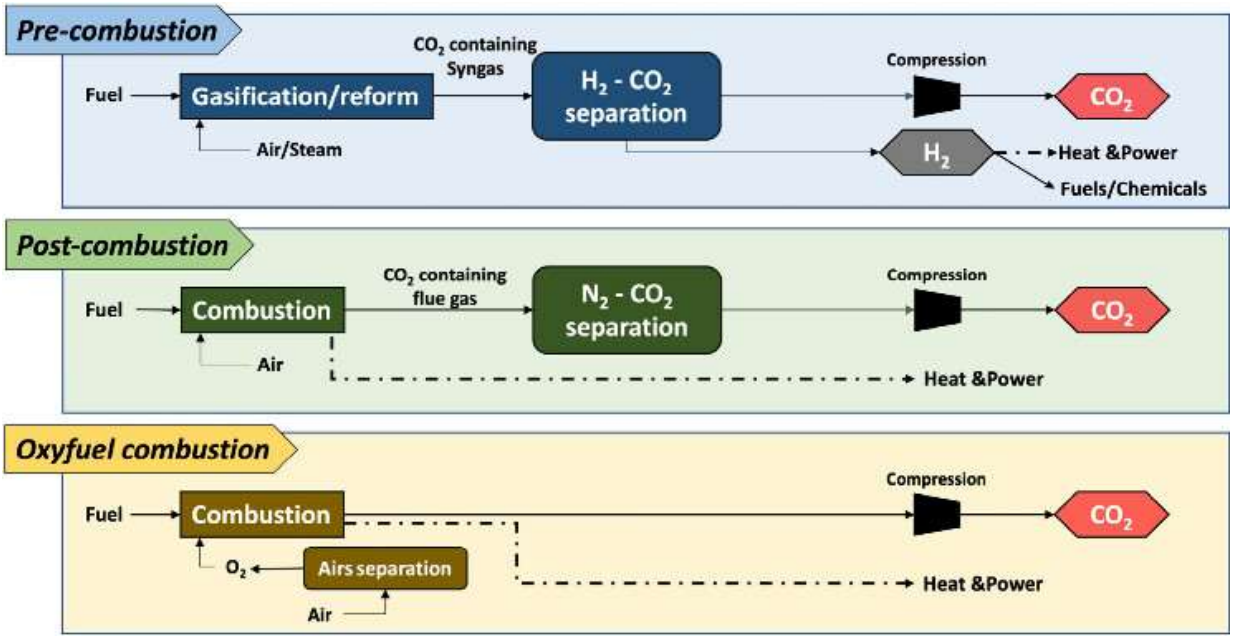

Figure 9 - The differences between pre-combustion, post-combustion and oxyfuel combustion processes [14]

The main separation techniques used for the CO_2 removal are absorption, adsorption, membrane separation and cryogenic distillation [13].

- **Absorption**: carbon dioxide is absorbed by a liquid solvent, either just dissolving physically or chemically reacting. The process is very effective and commercially proven, but the regeneration of the solvent requires a lot of energy.
- **Adsorption**: a solid adsorbent captures the molecules with physical forces or chemical reactions. Some of the most used ones are activated carbon, Zeolites and Metal Organic Frameworks (MOFs). They require less energy than liquid solvents, but the capturing capacity is lower.
- **Membrane separation**: depending on the molecular sizes and solubility, different gas molecules pass through the membrane faster than other. The membrane can be polymeric, inorganic or a Mixed Material Membrane (MMMs). They require low maintenance and work continuously. Some of the disadvantages are the performance drop at low CO_2 concentrations and the trade-off needed between the speed and the selectivity of the process.
- **Cryogenic distillation**: the difference in the condensation or sublimation temperatures of different gases is exploited. The purity of the produced CO_2 is high but the process is strongly energy intensive, and it is efficient only with high CO_2 concentrations in the inlet flow.

1.5 Main renewable fuels of non-biological origin

In the following paragraphs some of the main renewable synthetic fuels are described. The e- before the fuel name indicates that they are green fuels produced with renewable hydrogen.

1.5.1 E-Methane

Methane (CH_4) is the main constituent of natural gas, accounting for 85-90 % of its total composition. It can be used for all natural gas applications and to power high temperature fuel cells (SOFC). Unlike hydrogen, it can be directly injected in current infrastructures, and it has almost a three times higher volumetric energy density than H_2, making it easier to transport and manage.

In the diagram below the possible steps involved in a Power to Methane process are represented.

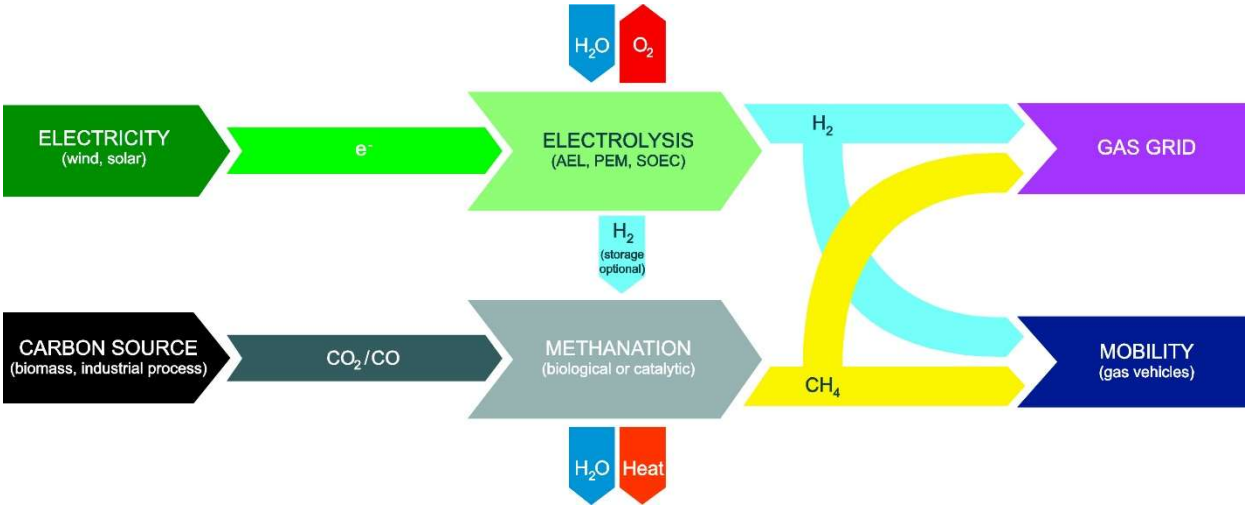

Figure 10 - The steps forming a Power to Methane process [11]

E-methane is produced by the hydrogenation of CO_2 or CO, using green H_2:

$$CO_2 + 4H_2 = CH_4 + 2H_2O$$
$$CO + 3H_2 = CH_4 + H_2O$$

This process is usually carried out with thermo-catalytic technologies, using Ni-γ-Al_2O_3 catalytic beds, but it can also take place in bioreactors through hydrogenotrophic methanogenesis.

Methane is also the main component of biogas, which is obtained through anaerobic digestion of biomass and wastes. Biogas can be directly used, or it can be exploited to produce biomethane, removing the CO_2 or causing a reaction with hydrogen produced with electrolysis. In this last case it falls again under the category of e-methane.

1.5.2 E-Methanol

Methanol is the simplest alcohol, and its formula is CH3-OH. Compared to hydrogen or methane, its main advantage is that it is in liquid form at ambient conditions and so it is easier to store and transport. It is often used to produce other chemical compounds like formaldehyde and acetic acid, but it can be used as a fuel, for example in gasoline internal combustion engines, with minimal modifications.

Renewable methanol can be produced starting from green hydrogen and biomass or captured CO_2, as visible in the following equation:

$$CO_2 + 3H_2 \rightarrow CH_3OH + H_2O$$

The reaction takes place at a temperature of 230-270 °C and a pressure of 50-70 bar. The catalysts used are CuO and ZnO, in most cases on a carrier of Al_2O_3, with variable stabilising additives and promoters like Zr, Cr, Mg and rare earth metals.

Through methanol dehydration, dimethyl ether (DME) can be produced:

$$2CH_3OH \rightarrow (CH_3)_2O + H_2O$$

DME is an interesting alternative as a fuel for diesel engines and DME direct fuel cells have been developed and tested. It is also interesting because it is a precursor of kerosene, and it could be fundamental in the production of synthetic green fuels for airplanes.

1.5.3 E-Ammonia

Ammonia is the simplest nitrogen hydride, formed by an atom of nitrogen and three atoms of hydrogen, and it is gaseous at ambient temperature. It is widely used as a precursor for food and fertilizers and for the synthesis of many pharmaceutical products. It is also exploited as a fuel, even though it burns with difficulty in air.

The main process for ammonia production is the Haber-Bosch one: hydrogen and nitrogen react at high temperature (300°C-550°C) under high pressure (15-30 MPa), with a mixture of iron, potassium oxide and aluminium oxide as a catalyst.

$$3H_2 + N_2 \rightarrow 2NH_3$$

When the hydrogen is produced from a renewable source, the ammonia is considered green.

1.6 Gas networks legislations

Legislations regarding the specifics needed to inject a gas in the network are a crucial issue, as one of the main purposes of chemical and biological methanation is to obtain a synthetic methane that can be used as a substitute of natural gas. The properties of the produced gas are related to the gas composition and the ratio of the different gases present: the higher the presence of CH_4 is, the most similar the mixture is to the natural gas. For this reason, this parameter is fundamental to assess the performance of a methanation technology.

Usually, the technical requirements are set at a national level, but for example in the United States they are chosen by the pipeline operators or

set for interstate pipelines. The main parameters considered are the following:

- **Higher Heating Value** (HHV): it is the total amount of heat released by a unit of mass or of volume of the gas during the combustion, including the latent heat of vaporization of water produced during the process [15]. Usually it is expressed in MJ/Sm^3.
- **Relative density**: it is the ratio between the gas density and the air density, at standard conditions.

$$RD = \frac{\rho_{NG}(T_{std}, P_{std})}{\rho_{air}(T_{std}, P_{std})}$$

- **Wobbe Index**: it is one of the main indicators of gas fuels interchangeability and it is the ratio between the HHV and the square root of the relative density. Usually it is expressed in MJ/Sm^3.

$$WI = \frac{HHV}{\sqrt{RD}}$$

In some cases, along with limits on these parameters there are also rules regarding the ratio of the gases present in the mixture, especially in the case of hydrogen. For example, in Italy since 2022 the maximum concentration of hydrogen permitted is 2%.

In the table below the current limits present in some European countries are reported [16].

Country	**Max. Hydrogen doping ratio**
Finland	1%
Switzerland, Germany, Italy	2%
Austria	4%
Spain	5%
France	6%

However, in countries like Germany, France and the UK, portions of the current system are being tested and the results show that with small adjustments mixtures containing between 10 and 20% of hydrogen can be safely managed by the network [17]. The trend for the future is to build systems that can withstand high hydrogen ratios, as this gas is gaining more and more popularity because of its possible production with green electrolysis.

2. BIOMETHANATION

In the biological methanation process, molecular hydrogen and carbon dioxide in gaseous form are converted into methane by the work of specific bacterial groups. In the majority of cases the CO_2 comes from produced biogas and this process is used for biogas upgrading to biomethane, which can then be injected in the gas network or work as a fuel for vehicles or for electricity production.

2.1 In-situ and ex-situ configurations

There are two main reactor configurations, explained in Figure 11: in-situ and ex-situ. In the in-situ biomethanation, the hydrogen is directly injected in the same reactor in which the biomass is digested and the biogas is produced, while in the ex-situ one the hydrogen is mixed with carbon dioxide in a separate reactor.

The main advantage of the in-situ configuration is that the cost of the infrastructure is lower as the reactor used is the same in which the biogas production happens. However, the latest research and developments are more oriented towards the ex-situ technology. Being a separate process from the biogas production, there are fewer limitations related to the reactor's characteristics and internal conditions, and this leads to higher values of Methane Evolution Rate (MER). In the ex-situ process it is also possible to use any CO_2 source, making it a more flexible technology.

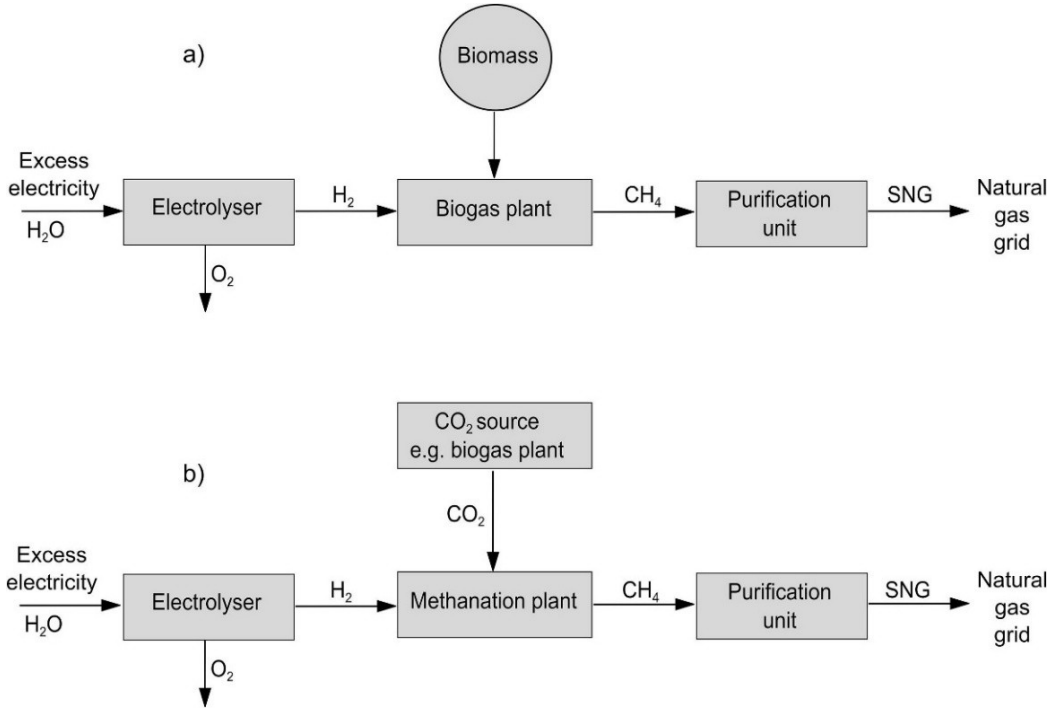

Figure 11 - The difference between in-situ (a) and ex-situ (b) configurations [18]

2.2 Biology

The most important microorganisms involved are Methanogenic bacteria, which are anaerobic microorganisms able to produce methane during their metabolism process. They are Archaea, belonging to the phylum Euryarchaeota. For greater clarity they can be divided in two categories: aceticlastic methanogens and hydrogenotrophic methanogens.

Aceticlastic methanogens are able to convert acetate into methane and carbon dioxide. The most important ones belong to the genera Methanosarcina and Methanoseta. Acetate can be metabolized from hydrogen and carbon dioxide by homoacetogens bacteria, via the Wood-Ljungdahl pathway. The homoacetogens are for example Acetobacterium woodii or species out of the microbial group Clostridia [19].

Hydrogenotrophic methanogens instead convert directly hydrogen and carbon dioxide into methane, using hydrogen as an electron donor. Until recently their involvement in biogas reactors was underestimated, while they actually have a key role in biogas production and so are strongly present in every biogas plant. Most hydrogenotropic bacteria belong to the methanogens group of Methanobacteriales, Methanococcales, Methanomicrobiales, Methanocellales, and Methanopyrales [20].

Figure 12 can help to have a better understanding of the bacteria's activity, along with the reported equations.

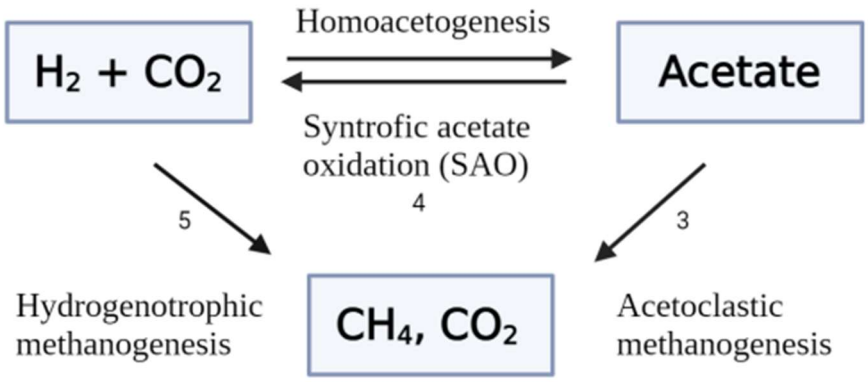

Figure 12 - Scheme of the reactions involving the different bacteria [21]

- Homoacetogenesis: $4\,H_2 + 2CO_2 \rightarrow CH_3COOH + 2H_2O$
- Acetoclastic methanogenesis: $CH_3COOH \rightarrow CH_4 + CO_2$
- Hydrogenotrophic methanogenesis: $CO_2 + 4H_2 \rightarrow CH_4 + 2H_2O$

The formation of both homoacetogenic and acetoclastic bacteria requires higher energy than the one the hydrogenotrophic bacteria and, according to Cazier et al. [22], methanogenesis is the more favored process

with respect to homoacetogenesis when H_2 and CO_2 are added inside a reactor. Because of the smaller Gibbs free energy drop, homoacetogenic bacteria also need the presence of a higher hydrogen concentration than the hydrogenotrophic ones, as stated by Taspekos et al. [23].

2.3 Reactor types

In the following paragraphs the main reactor technologies used for biomethanation are briefly described.

2.3.1 Continuous Stirred Tank Reactor (CSTR)

The reactor is fed with a continuous flow and equipped with a mechanical agitation system which makes the properties homogeneous inside it.

The goal of the intensive mixing is to make the gas bubbles as small as possible, to improve the gas-liquid mass transfer, one of the limiting factors for the reactor's performance.

This technology is widely used because it is relatively simple and cost-effective to put in operation.

The main issue is related to the energy consumed by the mixing mechanism and optional gas recirculation, used to improve the gas-liquid mass transfer.

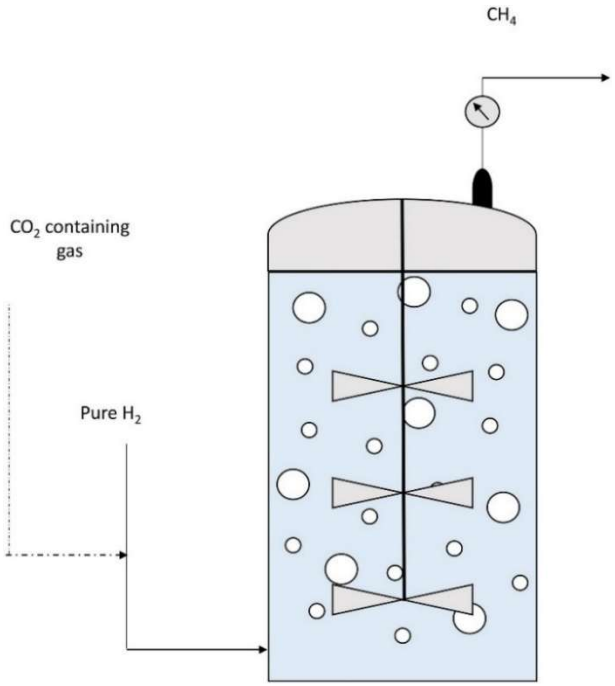

Figure 13. A continuous stirred tank reactor [24]

2.3.2 Bubble Column Reactor

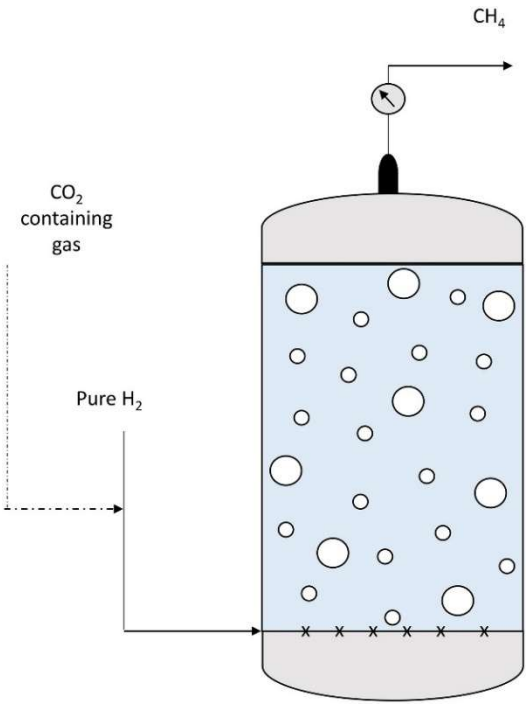

Figure 14 - A bubble column reactor [24]

In these reactors particular gas diffusers are used to inject small bubbles, to obtain a high volumetric interfacial area and increase the gas-liquid mass transfer coefficient. The up flow of the bubbles creates a convective motion which limits the stagnation areas inside the tank. One of the advantages is that the use of non-mechanical mixing leads to cheap operational costs.

2.3.3 Trickle Bed Reactor (TBR)

This reactor is loaded with gas instead of liquid and it is characterised by a pillar filled with a porous packing material where the microorganisms are immobilized.

The nutrient for the bacteria trickles down from the top, forming a liquid film around the surface of the packing material.

This minimizes the gas-liquid mass transfer restrictions and leads to high efficiency in the methane production, without the large energy consumption caused by continuous mixing or bubbling systems.

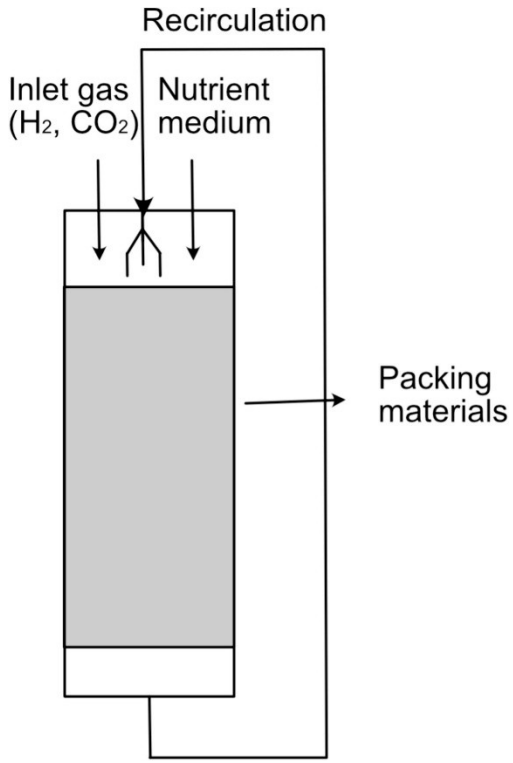

Figure 15 - A trickle bed reactor [25]

Many technical parameters still have to be optimized but nowadays it is considered as one of the most promising technologies for biomethanation.

2.3.4 Membrane Reactor

In this configuration, the gas is introduced through a hollow fiber membrane, which is characterized by small pores and allows fast gas-liquid mass transfer.

Some issues are the cost of the membrane when high surface is needed and the risk of clogging of the pores due to the creation of a biofilm by the microorganism.

The biofilm can have either a beneficial or a detrimental role, depending on the application.

2.4 Gas-liquid mass transfer

The gas-liquid mass transfer is a fundamental process that has a major impact on the efficiency of the reactor, as it limits the rate at which methane can be generated. The diffusion of the hydrogen inside the liquid is described by the two-film theory, where the bulk gas layer is separated from the bulk liquid layer by stagnant gas and liquid films present at the interface, as it can be seen in Figure 16. In the diagram P_g is the H_2 partial pressure in the bulk gas, $P_{g,I}$ is the partial pressure at the gas-liquid interface, $C_{l,I}$ is the H_2 concentration at the gas-liquid interface and C_l is the H_2 concentration in the bulk liquid.

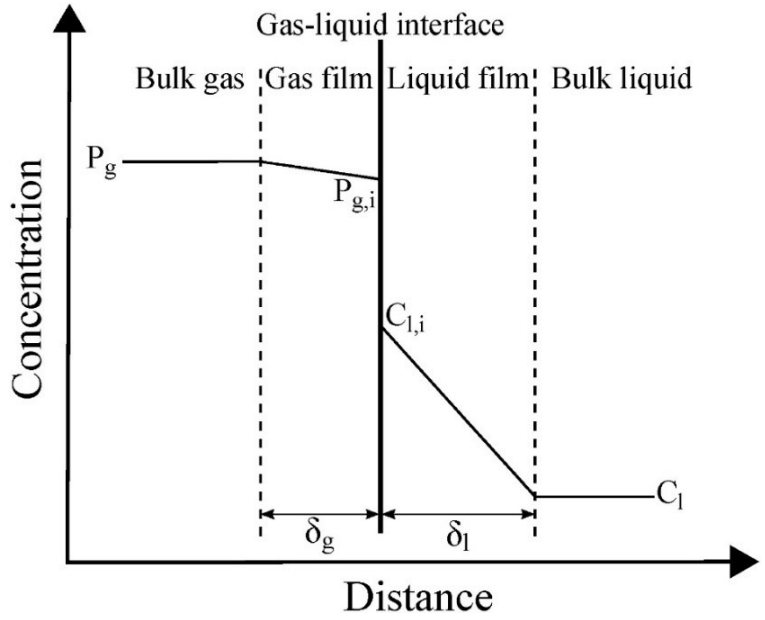

Figure 16 - Diagram describing how the concentration varies in space [26]

In the bulk gas and bulk liquid areas the concentration is considered homogeneous because of the convective motions happening in these parts, while in the stagnant layers there is a concentration gradient related to molecular diffusion. The system is considered to be in steady state

conditions and the H_2 flux going from bulk gas to bulk liquid is the same as the one in each of the films.

To relate the bulk gas partial pressure with the concentration of dissolved gas in equilibrium with it, Henry's law can be used, assuming the aqueous state as diluted and the gas as an ideal gas:

$$C_l^* = P_g / K_H$$

- K_H is Henry's constant [atm m^3 / mol]
- P_g is the gas partial pressure at the gas-liquid interface [atm]
- C^*_l is the dissolved gas concentration at the gas-liquid interface [mol/m^3]

The flux can now be computed with Fick's law:

$$r_{g-l} = K_l * a * (C_l^* - C_l)$$

In the formula above,

- r_{g-l} is the volumetric gas-liquid mass transfer rate [mol / (m^3 s)]
- a is the volumetric gas-liquid interfacial area [m^2/ m^3]
- K_l is the liquid-side volumetric mass transfer coefficient [m / s]

The value of K_l*a (kla) depends on the reactor's configuration. In Continuous Stirred Tank Reactors (CSTR), stirring and gas recirculation technologies are used to increase the gas-liquid mass transfer coefficient.

The effect of agitation can be calculated using Van't Riet correlations, described by the following formula:

$$(K_l * a) = A * \left(\frac{P_W}{V}\right)^B * V_S^C$$

- P_w is power consumed for agitation [Watt]
- V is the volume of the reactor [m^3]

- v_s is the superficial gas velocity [m / s]
- A, B, and C are empirical constants

It can be easily seen how the coefficient's value increases with the power consumed by the stirring device. Gas recirculation contributes to this increase by permitting a longer time of interaction between the gas and the liquid.

In bubble column reactors the mass transfer coefficient reaches a high value thanks to the gas diffusers which create small bubbles and so a high volumetric interfacial area, while in trickle bed reactors this result is obtained thanks to the high porosity of the packing materials.

2.5 Working conditions

2.5.1 Temperature

The temperature inside the reactor must be suitable for the methanogenic bacteria and so it is kept in the mesophilic (30–45 °C) or thermophilic (50–70 °C) range.

When the temperature increases, the solubility of H_2 inside the liquid decreases and so the gas-liquid mass transfer rate should decrease.

However, experimental studies, like the ones of Pokorna et al. [27] and of Zhu et al. [28], show that in thermophilic conditions the methane production rate is higher.

This happens because the methanogens' activity increases and creates a higher concentration gradient between the gas and the liquid, keeping consistent the gas-liquid mass transfer rate.

2.5.2 H_2 partial pressure

The hydrogen concentration in the reactor is chosen depending on the desired digestion speed and percentage of methane at the outlet, keeping in mind that a compromise is needed to have satisfying values of both.

In in-situ reactors, the hydrogen partial pressure is a delicate matter, because H_2 can damage the equilibrium of the many processes constituting anaerobic digestion.

In particular, acetogenic bacteria are hydrogen producers and their metabolism is inhibited by hydrogen: this can cause an accumulation of Volatile Fatty Acids (VFAs), like Propionate and Butyrate. Mulat et al. [29] and Wahid et al. [30] encountered this problem when they injected hydrogen in excess, surpassing the stoichiometric ratio of 4:1 with the CO_2.

For ex-situ reactors the upgrading takes place in a separate unit and so there isn't the issue of interfering with the biomass digestion processes, but an incorrect concentration of hydrogen can create an unsuitable environment for the microorganisms.

2.5.3 pH

In this type of reactors, it's important to keep the pH level in a certain range, usually between the values of 6.5 and 8.5 [31].

Different values can cause the inhibition of the microorganisms' digestion and damage the biological system.

Events like an accumulation of VFAs can produce a shift from the optimal values and in these cases it's necessary to actively modify the pH

level. For example, the injection of H_2 and CO_2 can be adjusted to keep it between the chosen thresholds.

At the pH levels mentioned before, most of the CO_2 inside the liquid phase is separated as shown in the equation below:

$$H_2O + CO_2 = H^+ + HCO_3^-$$

When the CO_2 is injected, the concentration of H^+ increases and so the pH decreases.

2.6 Commercial applications

Despite being a technology that still has to be fully developed, some companies are starting to distribute these systems at a commercial level.

Between them, one of the most important is Electrochaea GmbH, that specialises in ex-situ biomethanation and has commercial scale plants or near-commercial references in Europe.

Their reactor works at 63° C and at a pressure of 10 bar, producing grid-quality, certifiable e-methane. The specifications of their suggested biomethanation plants are summarized in the table below [32].

Other companies that are moving towards commercial scale projects are Enosis France [33] and Kanadevia Inova [34].

	1 MWe plant	10 MWe plant	50 MWe plant
Nominal gas input	200 Nm^3/h H2 50 Nm^3/h CO2	2000 Nm^3/h H2 500 Nm^3/h CO2	10000 Nm^3/h H2 2500 Nm^3/h CO2
Electrolyzer power requirement	1 MWe	10 MWe	50 MWe
Nominal outputs: - Grid quality gas - Thermal energy - Metabolic water	 50 Nm^3/h CH4 130 kWth 80 l/h	 500 Nm^3/h CH4 1275 kWth 800 l/h	 2500 Nm^3/h CH4 6400 kWth 4000 l/h
Energy conversion efficiency - H2 to CH4 conversion -Total system	 >74% 52-58%	 >74% 52-58%	 >74% 52-58%
Footprints (excluding electrolyzers)	150 m^2	480 m^2	1070 m^2

3. EXPERIMENTAL ANALYSIS OF AN EX-SITU REACTOR

An ex-situ biomethanation reactor at laboratory scale was studied, collecting the data concerning its operation every day. The data were then used to verify the functioning of the virtual model discussed in the next chapter.

3.1 Reactor's specifics

The reactor analysed is a laboratory scale fully mixed reactor used to collect data on the ex-situ biomethanation process in the mesophilic temperature range. The system works under fed batch conditions, meaning that there isn't a continuous flow of hydrogen entering the reactor but separate injections, that allow the assessment of the efficiency with different concentrations of nutrients.

A picture of the system is shown below.

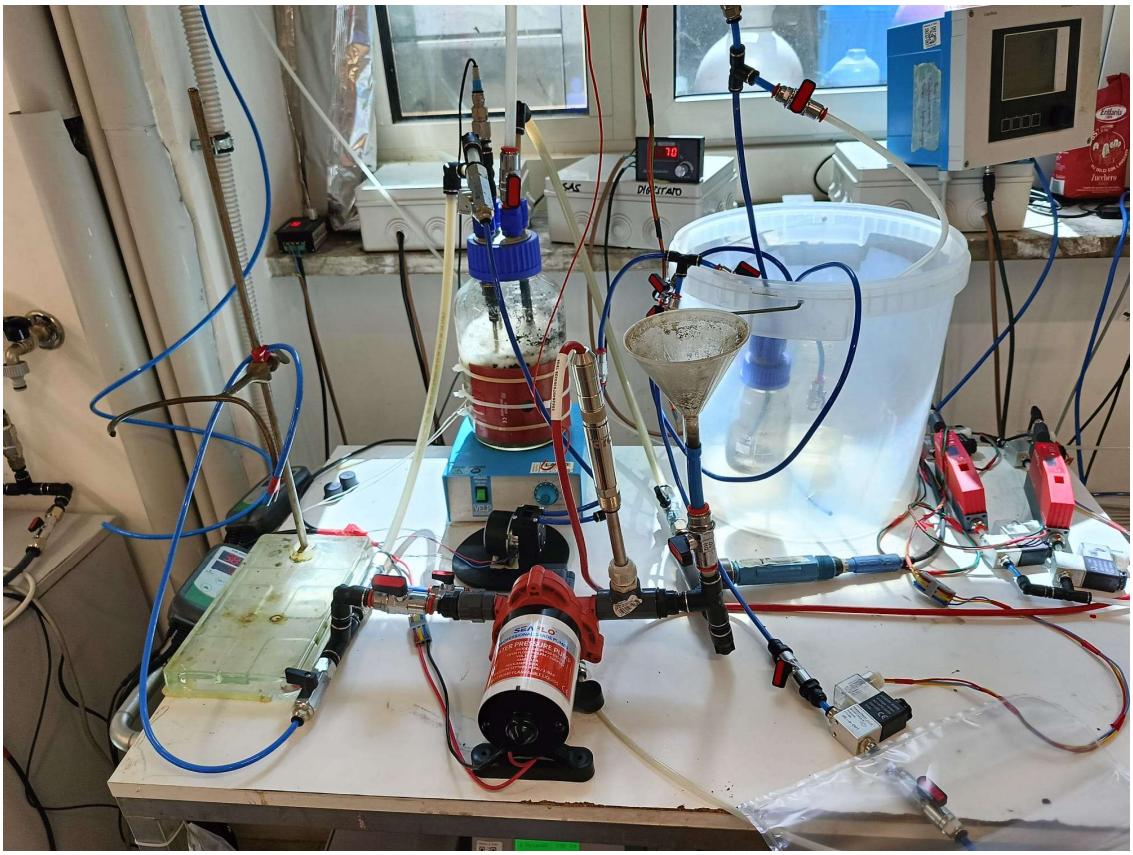

Figure 17 - The reactor used in the laboratory

The liquid is kept inside a 2.6 L Schott bottle and occupies a volume of 1.4 L. The inoculum consists of digested sludge taken from a wastewater treatment plant, necessary to have a sufficient concentration of hydrogenotrophic bacteria, the ones responsible for the chemical process characterizing the system.

The temperature is kept at 38 degrees Celsius by a thermostat control based on an electric resistance.

To assure a good gas-liquid mass transfer, the liquid is taken from the bottom of the bottle and re-injected in the top part by a water pump, creating intense mixing inside the reactor. An additional feature with the same purpose is a rotating magnet placed on the bottom.

The injection of hydrogen and carbon dioxide is regulated by electrovalves and happens thanks to a diffuser similar to the ones used in aquariums. Hydrogen is directly produced in the laboratory thanks to a small electrolyser while carbon dioxide is bought on the market.

To monitor the inside conditions instant by instant a series of sensors are used: a pressure sensor, a pH sensor, a CO_2 concentration sensor and a temperature sensor. The CO_2 concentration sensor and the pH sensor are placed in the circuit of the water pump while the pressure sensor is placed above the reactor in the circuit filled by the gas part. The temperature sensor is instead positioned inside the reactor.

The system is managed by a Matlab code running on a pc, connected with the electrovalves thanks to an Arduino board. The main parameter which regulates the gas injection and removal is the pressure. The cycle that repeats is the following: beginning with a pressure of 100 mbar (over atmospheric pressure), at first hydrogen is injected until a pressure of 400 mbar is reached, then the methanation starts and the pressure decreases to a value of 175 mbar, that triggers the removal of the produced gas and causes the overall pressure to drop down to the initial value of 100 mbar. Four of these series are shown in the diagram below.

The pressure decreases during the methane production because, as it can be seen in the chemical reaction, from 5 initial moles of gas (4 of hydrogen and 1 of carbon dioxide) only 1 mole of gas is produced, in form of methane. Carbon dioxide is injected in small steps during the cycle, depending on the concentration detected by the sensor. The overall ratio between hydrogen and carbon dioxide injected should be 4:1 if the system is working correctly and the organic materials concentrations are constant. The pressure values that regulate the opening of the valves are chosen to respect this ratio.

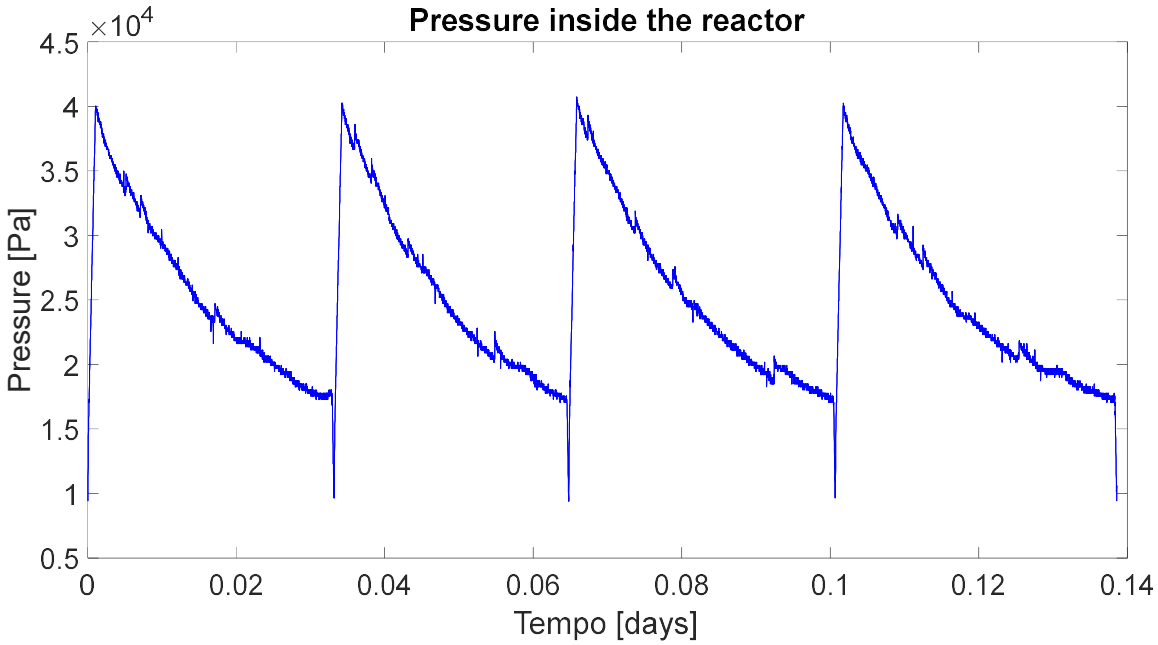

Figure 18 - Example of the cycle happening inside the reactor (17 March 2025, from h 18:32:23 to h 21:51:49)

The discharged gas is stored inside polyvinyl fluoride bags that are exchanged daily. The gas inside the bag is analysed with gas chromatography to obtain the concentration of CH_4, CO_2, H_2, O_2 and N_2 and its volume is measured.

On the pump circuit two outlet valves are present, to allow the removal of samples of liquid to test. To keep the liquid volume constant, tap water or digestate is inserted depending on the needs of the reactor.

3.2 Collected data

Many data were collected by the sensors and stored by the PC inside Matlab files, but also laboratory tests were executed every day to analyse the gas produced and the microorganisms' concentration. The experimental phase lasted from 13 March 2025 to 8 April 2025 and from

26 May 2025 to 8 July 2025. At the start of the first period, the reactor was already working in the same conditions for some time, and it was possible to obtain stable data, with few issues encountered. On 8 April the system was shut down, and the liquid was put inside a fridge to preserve its organic composition. One of the goals was to see if it was possible to do so without having any fallouts later when the experimental work resumed. Maintenance and cleaning work were needed: all the plastic tubes of the different circuits were replaced, and a new pump was installed, along with a new CO_2 sensor. When the reactor was turned on again, the original idea was to allow hydrogen injections only in certain periods of the day, to simulate the intermittence of hydrogen production with renewable energies and see how much this affected the efficiency of the system. Because of a series of issues encountered that are going to be explained later, this approach was tried only on a few occasions.

The quality of the biomethanation technology can be evaluated considering two parameters, the MER and the methane content. The Methane Evolution Rate (MER), usually expressed in $Nm^3/(\ Nm^3$ day), is related to the production's speed and it quantifies how many Liters of gas are produced in a day by a one Liter volume part of the reactor. If the MER value is satisfying, the other main requirement is to have a sufficiently high methane content in the exit gas, in order to complain with the regulations and have a gas with many possible uses. Other needs are obtaining a high hydrogen utilization efficiency and low energetic end economic expenses related to the functioning of the reactor.

The problem is that the increase of one of these values often leads to the decrease of another one. For example, to have a high percentage of methane in the exiting gas a high gas retention time is needed but this leads to a low MER. Another way to improve the quality of the exiting gas is to work on the gas liquid mass transfer, by increasing the pressure

inside the reactor or the speed of the mixing mechanism: this however causes higher energy consumptions and higher overall costs.

3.2.1 Time interval: 13/3/2025 - 8/4/2025

During this period, 150 ml of liquid were removed daily from the reactor to perform analyses, and they were replaced with 150 ml of digestate coming from a small biogas digester present in the laboratory. For this reason the Hydraulic Retention Time (HRT), which defines how many days the liquid remains inside the reactor, remained constant and equal to 9.33 days. The insertion of digestate instead of tap water was necessary to avoid a gradual washout of the system and to keep the conditions constant.

The following diagrams show the composition and the volume of the gas produced. Some days are missing because of practical issues that altered the data collected.

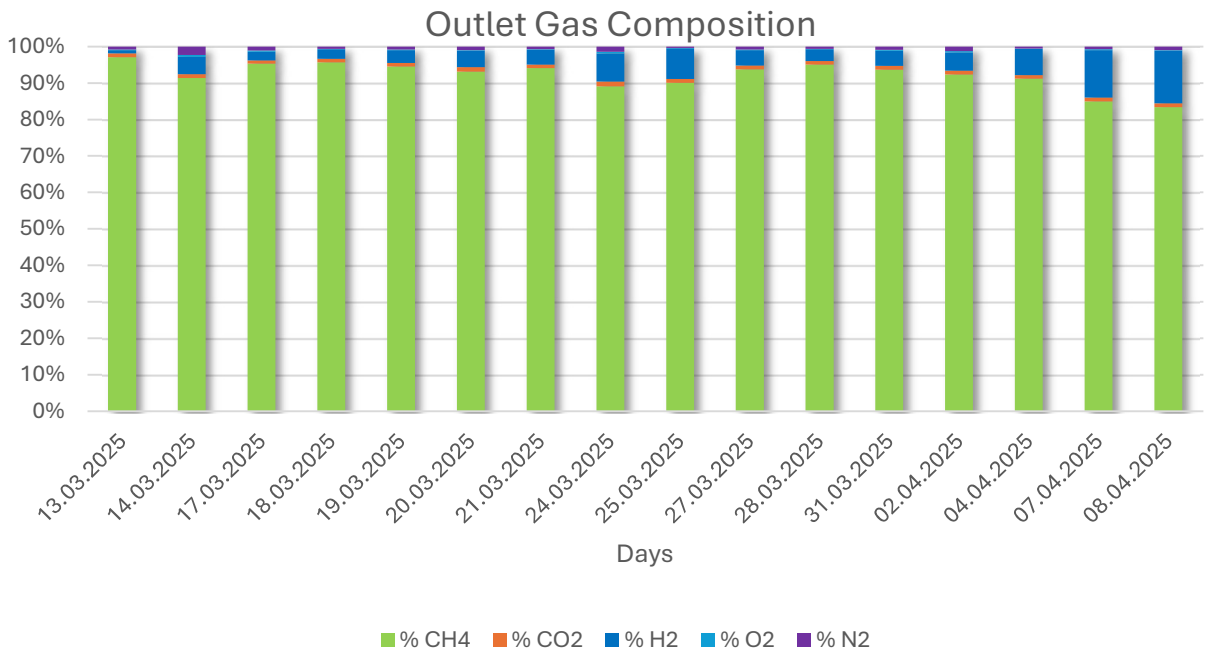

Figure 19 - Daily outlet gas composition

As it can be seen in Figure 19, high methane content is reached in the outlet gas, with an average value of 92.16 %. The remaining part is made on average by 5.62 % of hydrogen, 1.04 % of carbon dioxide and low values of nitrogen and oxygen. The scarcity of the last two shows that anaerobic conditions are kept inside the system.

From the values reported in Figure 20, an average MER of 3.59 $Nm^3/(Nm^3 days)$ is obtained.

To determine the processes happening inside the reactor, different tests were executed on the daily samples.

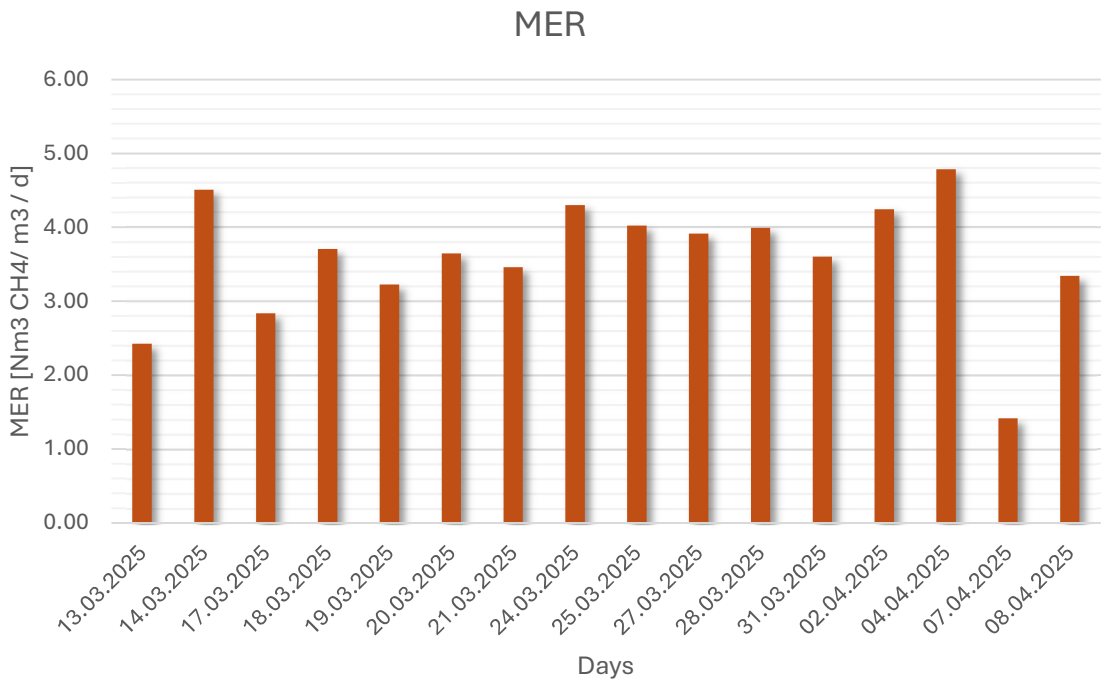

Figure 20 - Daily Methane Evolution Rate [Nm3 $CH4$/ m3 / d]

The pH was constantly monitored on the Matlab script using the pH sensor, but the pH values of the samples were also collected during the FOS/TAC test. From the diagram in Figure 21 it can be seen that they remain approximately constant, diminishing slightly during the last period.

This happens also thanks to the pH control systems present in the Matlab code, that avoids the crossing of a threshold regulating for example the carbon dioxide injections.

The average value recorded is 8.1, which is near the upper limit for the optimal growth of hydrogenotrophic bacteria.

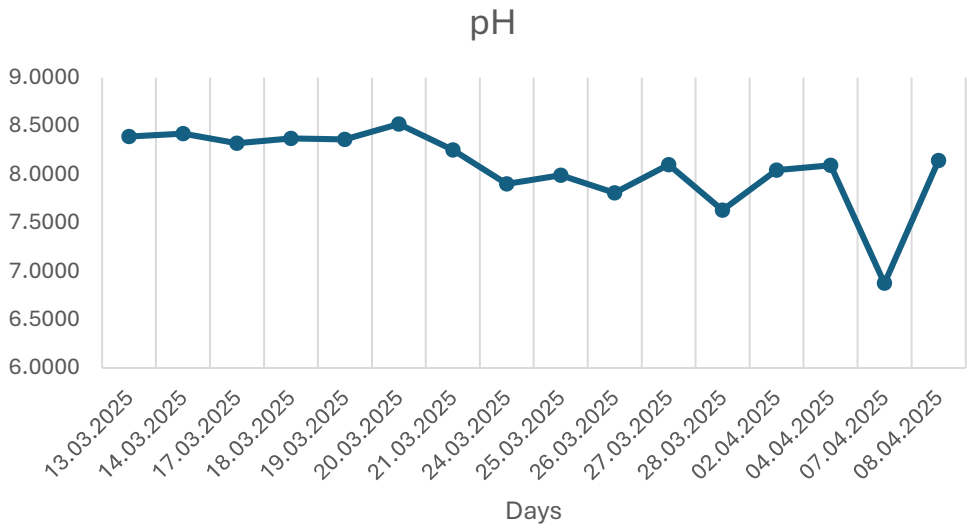

Figure 21: pH trend

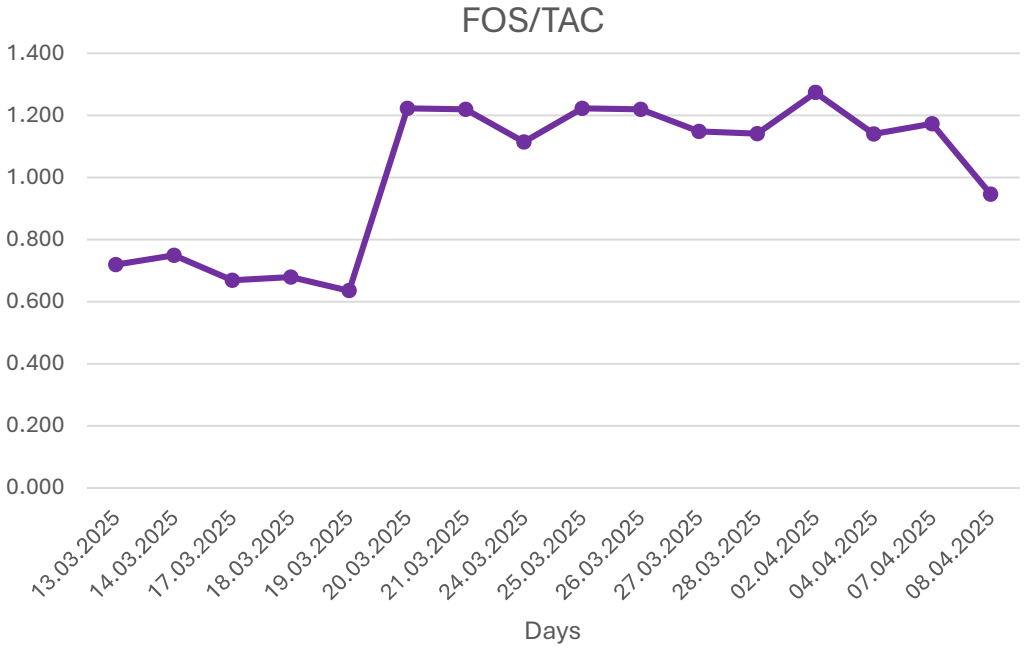

Figure 22: FOS and TAC trends

In the diagram in Figure 22 FOS and TAC values are reported. The FOS (Free Organic Substrates) is related to the quantity of organic carbon sources that the microorganisms can consume in a standard biogas reactor. Here it is mainly useful to monitor the accumulation of Volatile Fatty Acids (VFA). The TAC (Total Alkalinity Capacity) refers to the buffering capacity of the system, indicating how resistant it is to pH changes. The TAC is useful to check if the methanogens community is stable and if the system has enough buffering capacity to neutralize the VFAs. The collected data show relatively stable values of FOS, while the TAC values decrease.

To draw conclusions, it necessary to analyse also the FOS/TAC ratio trend, visible in Figure 23.

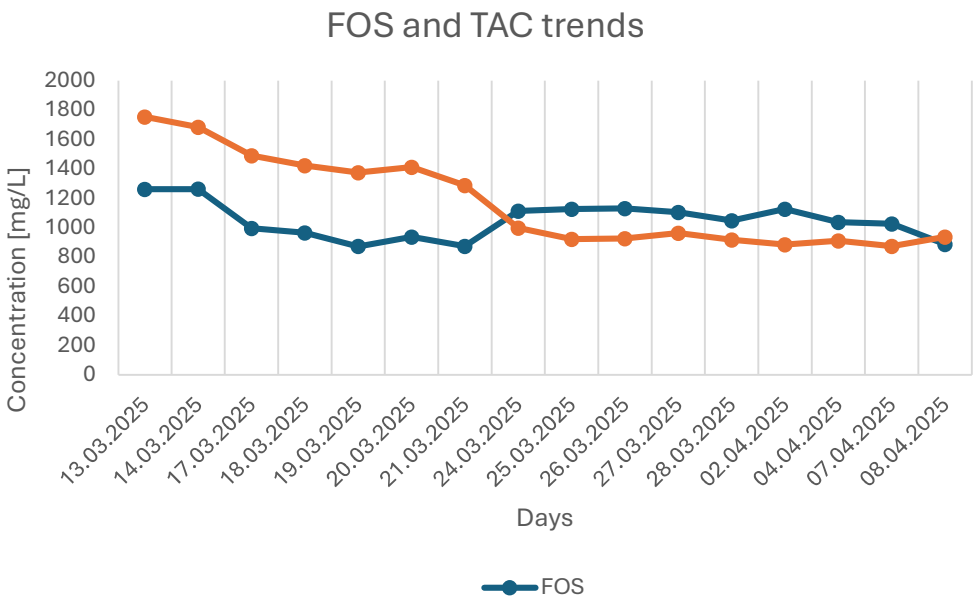

Figure 23 - FOS/TAC ratio

Looking at the graph, a sudden increase in the ratio is shown between March 19th and March 20th. It can be caused by VFAs accumulation, due to slower methanogenic work. The slight drop of the pH value started to

happen at the same time, showing a correlation between the different types of data collected.

Chemical Oxygen Demand (COD) analyses were conducted to quantify the presence of organic material inside the reactor and to perform overall balances in terms of COD to check possible issues with the collected data.

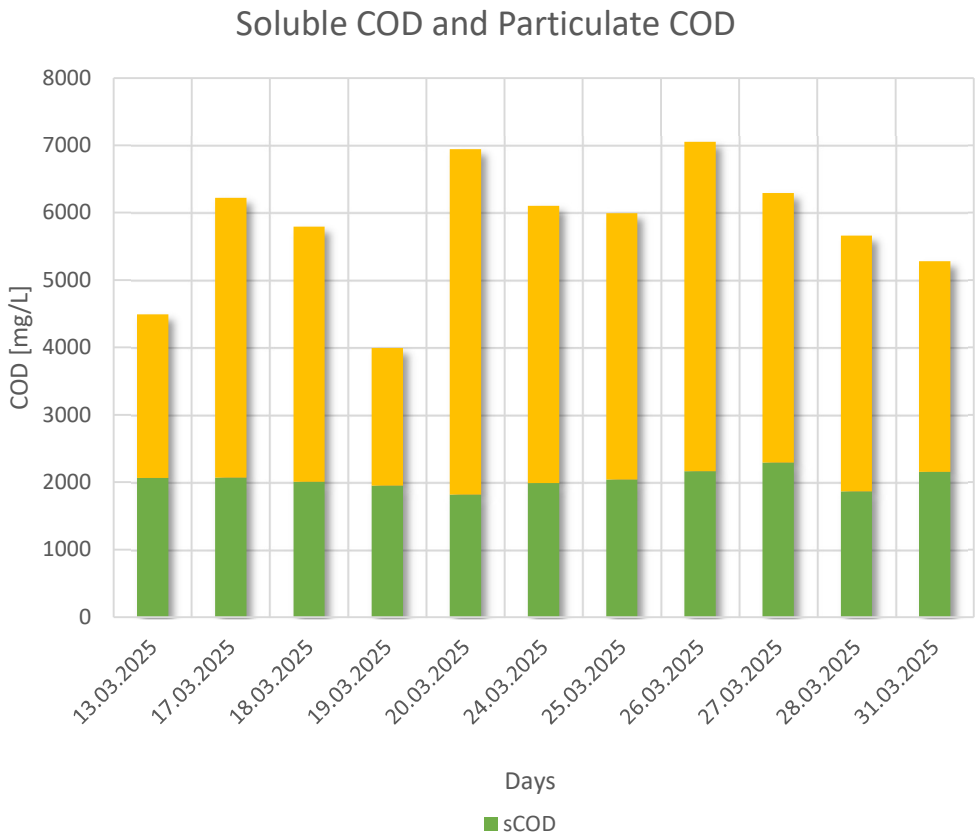

Figure 24 - Soluble COD and particulate COD [mg/L]

Figure 24 shows stable values of soluble COD, while the particulate COD values increase in the second half of the time period. The substantial increment between March 19th and March 20th happened with the previously discussed pH decrease and FOS/TAC ratio increase, and it can be related with VFAs accumulation.

3.2.2 Time interval: 26/5/2025 – 8/7/2025

After a few days of testing to check that the new components were functioning properly, on the May 26th the previous working cycle was resumed. At first slightly higher values were selected for the discharge pressure, allowing lower methane concentration in the outlet gas but avoiding the slow methanation happening at low pressures. In the following diagrams it can be seen how the collected values gradually became stable and similar to the ones taken during the first experimental period.

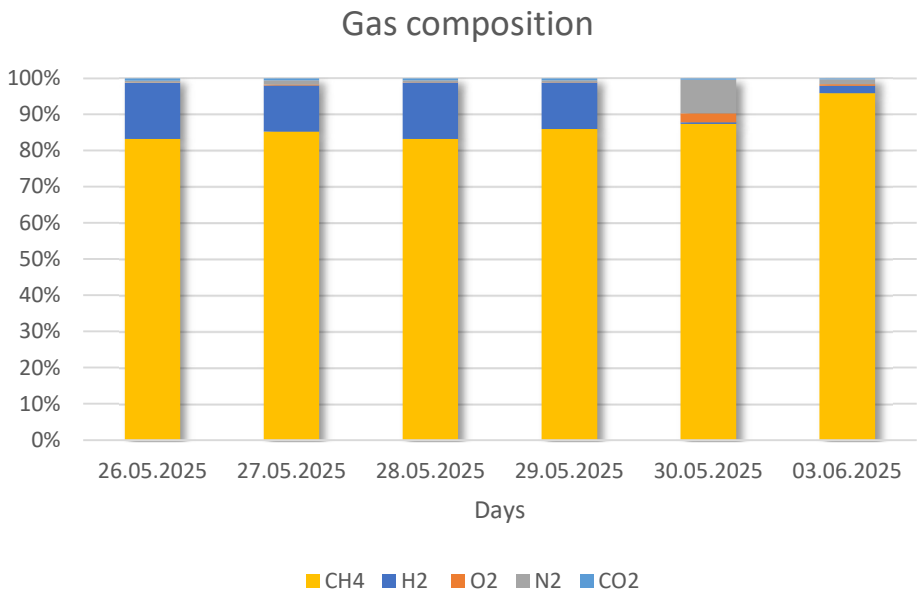

Figure 25 - Gas composition

Figure 25 shows how the methane content of the outlet gas increases and reaches a value of 95%. On 30 May some air entered in the system and caused a higher presence of nitrogen but it can be seen that the hydrogen was almost entirely transformed. At the end of this period the MER was equal to 3 $Nm^3/(Nm^3 days)$.

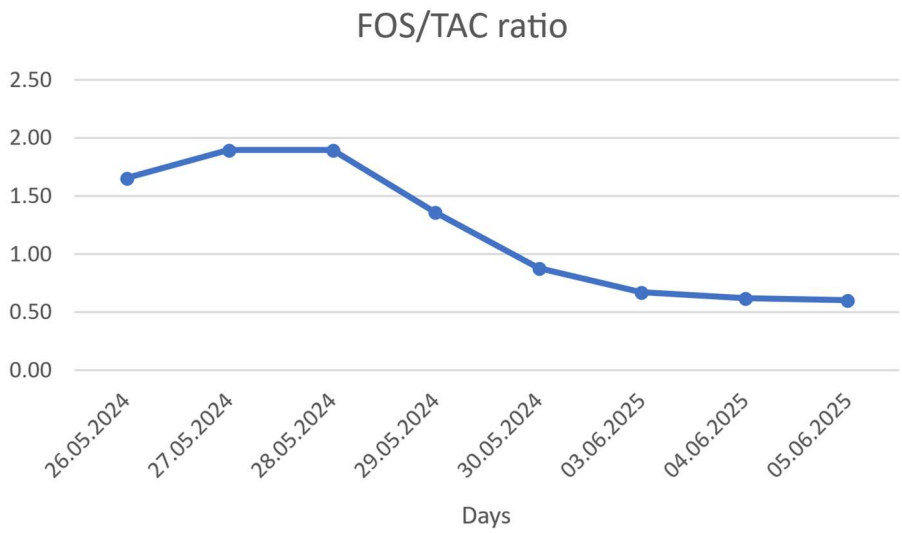

Figure 26 - FOS/TAC ratio

As reported in Figure 26, starting from values near to 2 the FOS/TAC ratio decreases and stabilizes around 0.6, as it happened during the other experimental interval of time. The high FOS/TAC ratio was probably related to VFAs accumulation caused by slow the slow work of the microorganisms at the start of the reactor.

Figure 27 shows relatively small changes in the soluble COD values and a drop of the particulate COD values. This could be related to VFAs accumulation, as it happened together with the drop observed in the FOS/TAC ratio.

On June 4th an electrovalve broke after overheating and in the following days the system also experienced a blackout and problems with the PC. For these reasons the regular working cycle was interrupted for 7-8 days while the reactor temperature was kept in the mesophilic range. When the gas injection began to happen regularly again, the microorganisms digested slowly, and low quantities of methane were produced.

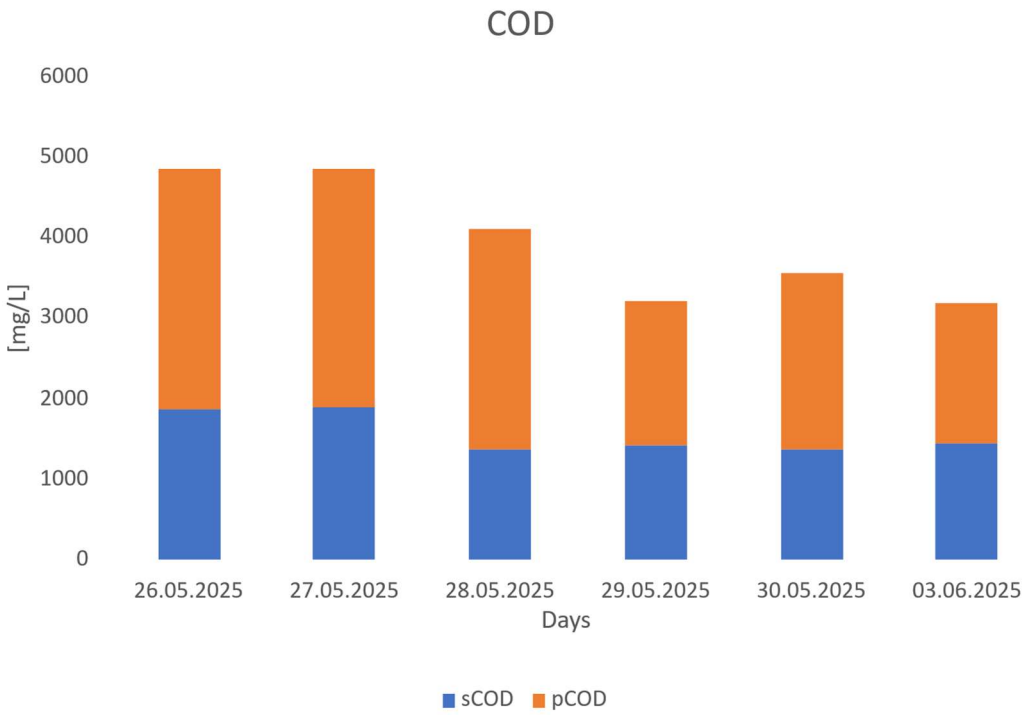

Figure 27 - Soluble and particulate COD

The best MER values obtained before stopping the reactor were only around 1.6 $Nm^3/(Nm^3 days)$ and only for a few days the methane quantity in the outlet gas exceeded 90%. The linear shape of the pressure curves suggested a low concentration of microorganisms, which leads to slow methane production.

Despite the slow digestion speed, a new method to regulate the carbon dioxide injection was researched. Until then the carbon dioxide injections were controlled depending on the values recorded by the CO_2 sensor, which is a very expensive instrument, and it is unable to consider the transformation into bicarbonate that the carbon dioxide undergoes in the pH range characterizing the reactor. This transformation was accounted for in the Matlab code, but for high pH values it is difficult to obtain reliable data using the sensor.

The new control method is based on the pH variations that the carbon dioxide causes when it enters or exits the liquid, discussed in the paragraph about the conditions inside a biomethanation reactor. When the CO_2 enters the solution, the pH decreases and so the goal is to keep the pH level stable to maintain a constant concentration of carbon dioxide. The issue encountered is that there are other factors which can affect the pH value of the solution, for example a temporary accumulation of VFAs. In this case, the system injects less CO_2 and the whole process slows down. If this happens for long periods it can cause an excessive reduction of the concentrations of hydrogenotrophic methanogens and affect the production for a long time.

For this reason, this method can be used only if the conditions are stationary and there are means to verify that the pH value is influenced only by the inorganic carbon concentration.

3.3 Overview of performances obtained in other systems

To evaluate the performance of the reactor, it's important to compare the results with others that can be found in literature for similar systems. Some examples are reported below.

Concerning CSTRs, Luo and Angelidaki [35] reached a CH_4 content around 95% with a MER of 3 $Nm^3/(Nm^3 days)$, after increasing enough the stirring speed and injecting a mixture of biogas and hydrogen. Voelklein et al. [36], thanks to a ceramic gas diffuser and a pump recirculating the gas for 24 h at a rate of 4 L/min, reached a CH_4 content around 96% and a H_2 utilization efficiency of 100%, achieving methane formation rates of 3.7 $Nm^3/(Nm^3 days)$.

With a bubble column reactor, Laguillaumie et al. [37] reached a methane concentration of 94% with a MER of 4 $Nm^3/(Nm^3days)$.

Using a trickle bed reactor, Rachbauer et al. [38] obtained a 96% methane concentration with a productivity of 2.52 $Nm^3/(Nm^3days)$, while Tsapekos et al. [39] reached a maximum methane content of 98.5 % with a gas retention time of 5 hours.

The data obtained from the laboratory reactor are perfectly comparable with the values reported above, showing that the system is on average working correctly.

4. VIRTUAL MODEL OF EX-SITU BIOMETHANATION

Starting from virtual models elaborated in the past, a model of the laboratory reactor is created on Simulink. In the following chapter its various sections are described, along with the equations involved. At the end the values of the parameters used are reported and explained.

To verify its correct functioning, the data discussed in the section before are considered and compared with the results of the simulations. The goal of the model is to assess the effect that the various parameters have on the methane production and to find the best conditions to optimize the process.

4.1 Anaerobic Digestion Model No. 1 and following developments

The Anaerobic Digestion Model No. 1 (ADM1) [40] is a mathematical model developed in 2002 by the International Water Association (IWA), to simulate and predict the processes happening inside an anaerobic digester. It has been since used as the foundation for many similar projects regarding biological reactors, as it takes into account all the digestion steps: disintegration, hydrolysis, acidogenesis, acetogenesis and methanogenesis.

24 dynamic state variables are defined, including soluble substrates and microbial populations. It is based on ordinary differential equations and some differential algebraic equations, describing Monod-type or first-order kinetics for microbial growth and degradation. Some downsides are the

complexity of the model, caused by the many parameters involved, and the presence of variables difficult to measure practically.

The reactions considered are divided into two categories: biochemical and physico-chemical reactions. The first ones are catalysed by intra or extracellular enzymes and act on the pool of biologically available organic material, through biomass degradation, growth or decay. The physico-chemical reactions instead are not biologically mediated and describe ion exchanges and the gas-liquid mass transfer.

The space inside the reactor is divided into a liquid and a gas phase, which exchange molecules during the gas liquid mass transfer processes. Inlet and outlet liquid flows are considered, as well as an outlet gas flow to remove the produced gas. A scheme of this subdivision is reported below.

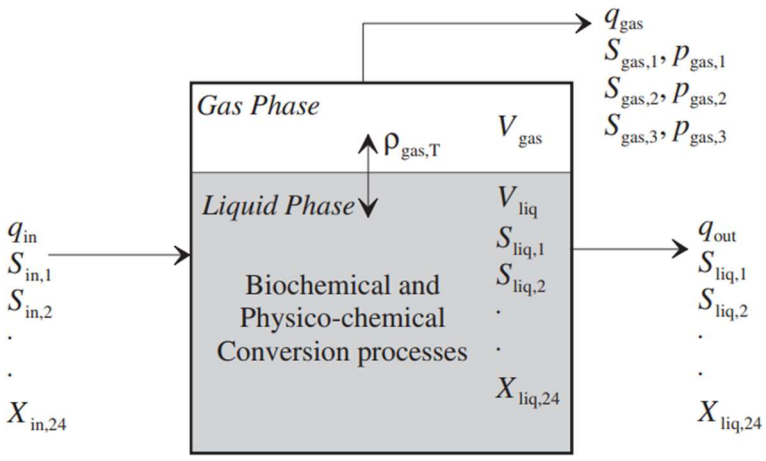

Figure 28 - Scheme of a digester based on the assumptions made in the ADM1 [40]

As steady state is reached in gas-liquid interactions, Henry's law is used to calculate the concentration of the molecules of the gases on the liquid surface, considered proportional to their partial pressures. The flows exchanged between the two phases are then calculated with Fick's law of

diffusion, that makes the fluxes proportional to the concentration gradient.

In 2005, Shang et al. [41] analysed the data collected from eleven wastewater treatment plant and confronted them with the results of simulations performed with the ADM1. The study shows that the model is a powerful tool to predict the steady state behaviour of full-scale plants, as in eight of the eleven cases analysed the results were predicted with a reasonable degree of accuracy, with the biogas yield being within 20% difference between the model and the collected data. In the other three cases the mismatch was probably due to questionable plant data and potential biogas meter malfunctions.

In 2022, Santus et al. [42] created a model for the simulation of ex-situ biogas upgrading. After modelling the equations, a sensitivity analysis was conducted and they identified the gas-liquid mass transfer coefficient of oxygen K_La_{O2}, the half-saturation constant on dissolved hydrogen $K_{S,H2}$ and the maximum specific uptake of hydrogenotrophic methanogens $k_{m,H2}$ as the most influential parameters for the methane production rate value. The mass transfer coefficient of Oxygen is considered because they calculated the coefficient for all the gases starting from the one of Oxygen.

Then they calibrated these parameters by experimental parameter identification, based on a Linear Fractional Transformation (LFT) reformulation of the model. As a last step, they tested the calibrated parameters with their own experimental data and with the ones of Bassani et al. [43], discovering that biogas composition and volumetric production have been well predicted by the model.

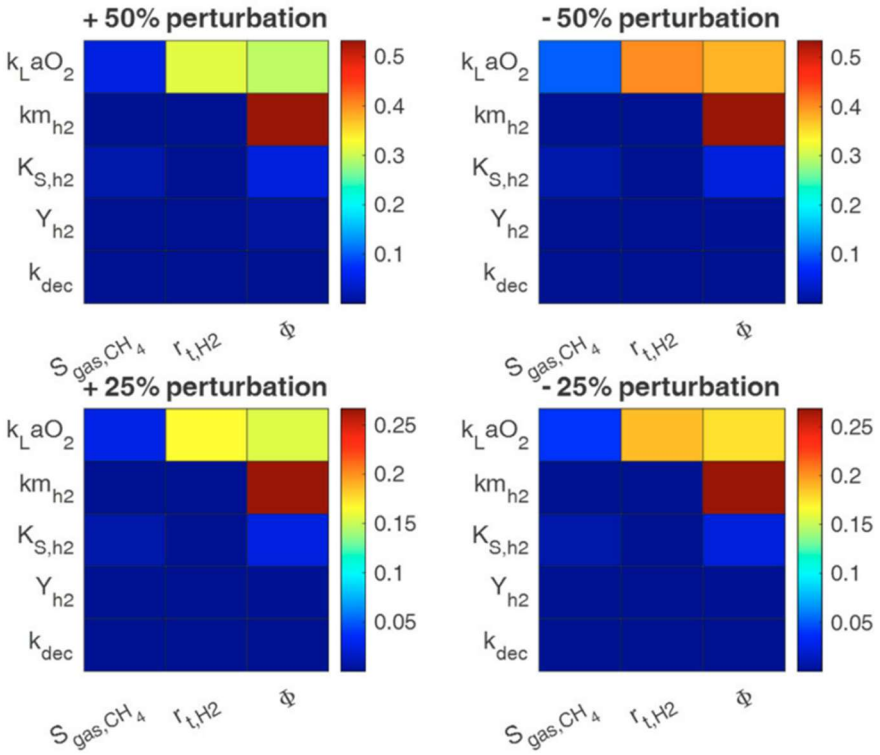

Figure 29 - The results of the sensitivity analysis conducted by Santus et al. [42]

Lovato et al. [44] conducted a sensitivity analysis on their model of an in-situ upgrading reactor and identified as well the kla as the most influential parameter for the upgrading processes.

In the diagram below, the results of the sensitivity are reported: the closer the column is to a PRCC value of 1 or -1, the higher the impact of the parameter is on the output variable.

A positive and a negative PRCC value mean a proportional and an inverse impact on the variable, respectively.

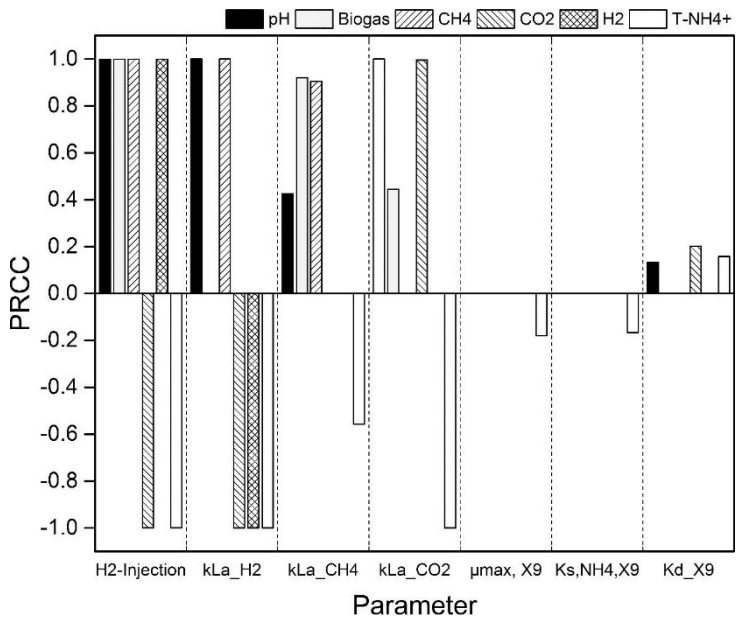

Figure 30 - The sensitivity analysis conducted by Lovato et al. [44]

4.2 Simulink model of ex-situ biomethanation

The goal of this work is to build a model on Simulink of an ex-situ batch fed reactor, to study the methane production mainly from the pressure behaviour in time, as it is the most significant parameter to analyse the processes happening in this type of reactors. Stationary conditions are considered, as the goal is not to study the evolution of the microorganisms during long periods of time.

The model can be seen as a simplified version of the Anaerobic Digestion Model No.1, as only the activity of hydrogenotrophic methanogens is considered, without the other steps of the anaerobic digestion. The other main difference is the presence of gas injections, which modify the equations describing the equilibrium in the headspace. The inhibition factor related to the pH, present in the ADM1, is not considered. As only short periods of time are simulated, the homoacetogenesis process doesn't cover a significant role and it is ignored.

This process is not included in the ADM1 but should be considered in models of biogas upgrading reactors, as the concentration of hydrogen is much higher. This eventually causes accumulations of VFAs, as a parallel reaction to the digestion of the hydrogenotrophic methanogens.

Unlike the ADM1 and the model by Santus et al. [42], the digestion speed of the microorganisms is regulated not only by the availability of the hydrogen substrate but also by the availability of the inorganic carbon substrate. For this reason, the product shown in the expression below is present in the biological equations.

$$\frac{S_{H2}}{K_{S,H2} + S_{H2}} \frac{S_{IC}}{K_{S,IC} + S_{IC}}$$

The concentrations of substrates are expressed by the terms S_{H2} and S_{IC}, while $K_{S,H2}$ and $K_{S,IC}$ are the semi-saturation constants, that indicate how much substrate the bacteria need to digest at the maximum speed. Each of the two terms of the equation can assume values that go from zero to one depending on the substrate availability. The value of $K_{S,IC}$ for hydrogenotrophic methanogens couldn't be found in literature and so it was taken from equations describing the growth of algae [45]. This doesn't really affect the system as the inorganic carbon concentration is never a limiting factor in the conditions considered.

At first, the laboratory reactor analysed in the chapter before is simulated, using its parameter as an input. To find its kla and the microorganisms' concentration X, a Matlab code is used to compare the curves of the pressure behaviour in time, simulated and experimental. The results are checked to make sure that they are similar to the one found in literature and the MER and methane concentration values obtained are compared with the ones collected in the laboratory.

Then a sensitivity analysis is conducted, to study the variations in the pressure curves shapes as the different parameters change, and the differences in the values of MER and methane presence in the output gas. Together with the kla and the microorganisms' concentration, the other main parameter considered is the pressure inside the reactor. At last, the best results achievable in the different configurations are summarized in tables.

4.2.1 Equations

In the following paragraph the structure of the model is analysed and all the equations used in the different subsystems are reported.

Valve opening and closing

A relay block regulates the hydrogen injection. It uses two given values as thresholds, that cause the switch ON and switch OFF of the block. The output is either 1 or 0 and it's modified using a gain block to obtain the value of the hydrogen flow. As the switch ON point must be higher than the switch OFF one, a gain block multiplies the pressure value entering by -1. As a result, the system injects hydrogen when the pressure goes under a chosen value, and it stops when the pressure overcomes the other threshold.

The same mechanism is used to regulate the CO_2 injections. Here the two thresholds are close as the goal is to keep the CO_2 concentration stable and never too low, as the system is studied with hydrogen as the limiting nutrient for the digestion speed.

The discharge valve is opened when the two conditions of the logic AND block are satisfied: the pressure must be below a threshold, and it must be decreasing in time.

Gas flow balances

In this subsystem there are the equations combining the entrance and the exit of the gases in the headspace. The gases considered are hydrogen, carbon dioxide and methane. To choose the initial concentrations, the values of the pressure and of the different concentration ratios are set. For each gas the following terms are summed: the gas injected from the outside (in the cases of H_2 and CO_2), the gas flow exchanged with the liquid phase depending on the concentration gradient and the gas removed during the discharging phase.

$$H2_{flow} = H2_{IN} - H2_{toLiq} - H2_{OUT}$$

$$CO2_{flow} = CO2_{IN} - CO2_{toLiq} - CO2_{OUT}$$

$$CH4_{flow} = CO2_{fromLiq} - CH4_{OUT}$$

In the case of hydrogen and methane, the units of measure of all the terms are kg COD/(m^3days), while in the case of carbon dioxide the terms are in kg IC/(m^3days).

To obtain the amount of gases present in the headspace the values of the flows are then integrated in time.

Pressure calculation

For the pressure calculation the gas quantities values are expressed in moles. Using the perfect gas equation the total pressure in the headspace is found:

$$P = \frac{n_{tot} RT}{V}$$

Using the temperature value expressed in K and the volume value in m^3, considering the gas perfect constant R equal to 8.314 (Pa m^3)/(mol K), the value of the pressure is found in Pa.

With the total pressure and the mole fractions, it's possible to obtain the partial pressure values, useful for the later calculation of the gas concentration inside the liquid:

$$P_i = \frac{n_i}{n_{tot}} P$$

Gas-liquid equilibrium

To estimate the concentration of the gases at the liquid interface, Henry's law is used. It describes the direct proportionality between the solubility of a gas and its partial pressure above the liquid:

$$C_{gas,i} = K_{H,i} P_i$$

$K_{H,i}$ is Henry's constant of the specific gas considered. It's important to notice that Henry's constant of hydrogen is much lower than the one of

other gases like CO_2. $K_{H,i}$ is expressed in mol/(m^3Pa), the pressure is expressed in Pa and the concentration is in mol/m^3.

Fick's law is used to calculate the specific flow of gas exchanged at the liquid interface, proportional to the concentration gradient between the two areas.

$$\dot{S}_{gas,i} = K_l a(C_{gas,i} - C_{liq,i})$$

$K_L\alpha$ is the gas-liquid mass transfer coefficient and is one of the most influential parameters in the regulation of the model. This coefficient is in 1/days, while the concentrations of hydrogen and methane are in kg COD/m^3 and the one of carbon dioxide is in kg IC/m^3. The gas flow is in kg COD /(m^3days) or kg IC /(m^3days) in the case of CO_2.

Biological equations

In this subsystem there are all the equations describing the activity of the microorganisms. With them it's possible to obtain the rate of consumption of the substrate and the variation of the microorganisms' population in time. The equations are reported below.

- $\frac{dS_{H2}}{dt} = \frac{qS_{H2,in}}{V} - \frac{qS_{H2}}{V} - k_{m,H2}\frac{S_{H2}}{K_{S,H2}+S_{H2}}\frac{S_{IC}}{K_{S,IC}+S_{IC}}X_{H2} + \dot{S}_{H2,gas}$

- $\frac{dS_{CH4}}{dt} = \frac{qS_{CH4,in}}{V} - \frac{qS_{CH4}}{V} + (1 - Y_{H2})k_{m,H2}\frac{S_{H2}}{K_{S,H2}+S_{H2}}\frac{S_{IC}}{K_{S,IC}+S_{IC}}X_{H2} - \dot{S}_{CH4,gas}$

- $\frac{dX_{H2}}{dt} = \frac{qX_{H2,in}}{V} - \frac{qX_{H2}}{V} + Y_{H2}k_{m,H2}\frac{S_{H2}}{K_{S,H2}+S_{H2}}\frac{S_{IC}}{K_{S,IC}+S_{IC}}X_{H2} - k_{dec}X_{H2}$

- $\frac{dS_{IC}}{dt} = \frac{qS_{IC,in}}{V} - \frac{qS_{IC}}{V} - 12C_{CH4}(1-Y_{H2})k_{m,H2}\frac{S_{H2}}{K_{S,H2}+S_{H2}}\frac{S_{IC}}{K_{S,IC}+S_{IC}}X_{H2} -$

  $12C_{bac}(Y_{H2}k_{m,H2}\frac{S_{H2}}{K_{S,H2}+S_{H2}}\frac{S_{IC}}{K_{S,IC}+S_{IC}}X_{H2} - k_{dec}X_{H2}) + \dot{S}_{IC,gas}$

The different parameters involved are described below:

S_{H2} = hydrogen concentration in the liquid [Kg COD/m^3]

S_{IC} = inorganic carbon concentration in the liquid [Kg IC/ m^3]

S_{CH4} = methane concentration in the liquid [Kg COD/ m^3]

X_{H2} = the concentration of hydrogenotrophic methanogens in the liquid [Kg COD/ m^3]

q = the volume of liquid entering and exiting the reactor each day [1/days]

V = the liquid volume inside the reactor [m^3]

$S_{H2,in}$ = hydrogen concentration in the liquid entering the reactor [Kg COD/ m^3]

$S_{IC,in}$ = inorganic carbon concentration in the liquid entering the reactor [Kg IC/ m^3]

$S_{CH4,in}$ = methane concentration in the liquid entering the reactor [Kg COD/ m^3]

$X_{H2,in}$ = the concentration of hydrogenotrophic methanogens in the liquid entering the reactor [Kg COD/ m^3]

$k_{m,H2}$ = maximum specific uptake rate of hydrogenotrophic methanogens [1/days]

$K_{S,H2}$ = hydrogen semi-saturation constant [Kg COD/ m^3]

$K_{S,IC}$ = inorganic carbon semi-saturation constant [Kg IC/ m^3]

Y_{H2} = growth yield of hydrogenotrophic methanogens [kg $COD_{X,H2}$ / kg $COD_{S,H2}$]

k_{dec} = first order decay coefficient of the biomass [1/days]

C_{bac} = carbon content in biomass [kmole C / kg COD]

C_{CH4} = carbon content in methane [kmole C / kg COD]

$\dot{S}_{H2}$ = specific flow of hydrogen entering the liquid [kg COD / (m^3days)]

$\dot{S}_{IC}$ = specific flow of inorganic carbon entering the liquid [kg IC / (m^3days)]

$\dot{S}_{CH4}$ = specific flow of methane exiting the liquid [kg COD / (m^3days)]

CO_2 - CHO_3 equilibrium

When carbon dioxide dissolves in water, a fraction of it reacts and forms carbonic acid H_2CO_3. When the pH overcomes a value around 6.3, carbonic acid becomes bicarbonate (HCO_3^-), while when the pH is over 10.3, carbonate (CO_3^{2-}) becomes the most diffused species. It's important to keep track of the concentrations of the different molecules as they have an impact on the flow of carbon dioxide entering the liquid from the gas, regulated by the concentration gradient. Due to the pH value of the liquid inside the reactor, the main species present are carbon dioxide and bicarbonate.

The formula allowing the calculation of the concentrations of bicarbonate and carbon dioxide are reported below:

$$[HCO_3^-] = \frac{[CO_2]K_a}{10^{-pH}}$$

$$[IC] = [HCO_3^-] + [CO_2]$$

The concentrations involved are expressed in kg IC/ m^3. Ka is the first acid dissociation constant of carbonic acid, and it is temperature dependent. This dependence is calculated with Van't Hoff temperature correction, as shown below.

$$K_{a,T} = K_{a,298} \exp\left(\frac{\Delta H}{R}\left(\frac{1}{298} - \frac{1}{T}\right)\right)$$

The different parameters involved are described below:

$K_{a,T}$ = first acid dissociation constant of carbonic acid at temperature T

$K_{a,298}$ = first acid dissociation constant of carbonic acid at a temperature of 298 K

R = gas constant [J/(mol K)]

ΔH = standard enthalpy change of the reaction, equal to 7646 [J/mol]

T = temperature at which the value of K_a is calculated [K].

MER and methane content calculation

To calculate the total methane collected from the reactor, the outlet gas flow is multiplied by the methane concentration in every instant, and the result is integrated by the total simulation time. Then to find the methane ratio in the total gas collected, this value is divided by the total gas collected, found integrating the outlet gas flow.

To calculate the Methane Evolution Rate (MER), the amount of methane gas collected is divided by the total time of the simulation. The MER value is then expressed in $Nm^3/(Nm^3 days)$.

4.2.2 Parameters' value

In this paragraph the value of each parameter in the model of the laboratory reactor is reported, along with an explanation of the reason behind it.

P_{min} = 100 mbar – minimum pressure in the laboratory reactor

P_{max} = 400 mbar – maximum pressure in the laboratory reactor

P_{dis} = 175 mbar – discharge pressure in the laboratory reactor

$H2_{inj}$ = 0.514 kg COD/days – flow of H_2 injected, approximately the value used in laboratory

$CO2_{inj}$ = 0.15 kg IC/days – flow of CO_2 injected, approximately the value used in laboratory

Discharge flow = 4.16 mol/days - approximately the value used in laboratory

$H2_{start}$ = 4% - initial H_2 concentration, chosen to start in almost stationary conditions

$CO2_{start}$ = 1% - initial CO_2 concentration, chosen to start in almost stationary conditions

$CH4_{start}$ = 95% - initial CH_4 concentration, chosen to start in almost stationary conditions

T = 310 K – value in the laboratory reactor

V_{gas} = 0.002116 m^3 – headspace volume, calculated with the perfect gas equation, knowing the moles of hydrogen injected in a time frame and the pressure change caused by their injection

V_{liq} = 0.0014 m^3 – liquid volume in the laboratory reactor

$K_{H, H2}$ = 7.8 * 10^{-6} mol/(m^3Pa) – Henry's constant for Hydrogen [46]

$K_{H, CO2}$ = 3.4×10^{-4} mol/(m^3Pa) – Henry's constant for Carbon Dioxide [46]

$K_{H, CH4}$ = 1.4×10^{-5} mol/(m^3Pa) – Henry's constant for Methane [46]

K_La = 5000 1/days - gas-liquid mass transfer coefficient, chosen a starting value before the optimization since the reactor is small and with intense mixing

q = 0 m^3/days – flow rate of liquid entering and exiting the reactor each day, equal to zero to work near stationary conditions

$k_{m,H2}$ = 35 1/days - maximum specific uptake rate of hydrogenotrophic methanogens, from ADM1 [40]

$K_{S,H2}$ = 7 * 10^{-6} Kg COD/ m^3 - hydrogen semi-saturation constant, from ADM1 [40]

$K_{S,IC}$ = 0.5 Kg IC/ m^3 - inorganic carbon semi-saturation constant [45]

Y_{H2} = 0.06 - growth yield of hydrogenotrophic methanogens, from ADM1 [40]

k_{dec} = 0.02 1/day - first order decay coefficient of the biomass, from ADM1 [40]

C_{bac} = 0.0313 Kmol C/kg COD - carbon content in biomass, from ADM1 [40]

C_{CH4} = 0.0156 Kmol C/kg COD - carbon content in methane, from ADM1 [40]

$H2_0$ = 2 * 10^{-8} Kg COD/m^3 – initial concentration of Hydrogen in the liquid, chosen to start in almost stationary conditions

IC_0 = 0.0177 Kg IC/m^3 - initial concentration of Inorganic Carbon in the liquid, chosen to start in almost stationary conditions

$CH4_0$ = 0.0132 Kg COD/m^3 - initial concentration of Methane in the liquid, chosen to start in almost stationary conditions

X_0 = 10 Kg COD/m^3 - initial concentration of Hydrogenotropic methanogens, chosen a starting value before the optimization

$K_{a,298}$ = $10^{-6.35}$ - first acid dissociation constant of carbonic acid at 298 K [47]

ΔH = 7646 J/mol - standard enthalpy change of the reaction of carbonic acid dissociation [48]

pH = 7.8 – average pH value in the laboratory reactor

4.3 Results of the simulations

To verify the correct functioning of the model, the data discussed in the chapter related to the experimental work are considered and compared with the results of the simulations. The goal of the model is to assess the effect that the various parameters have on the methane production and to find the best conditions to optimize the process.

4.3.1 Experimental curves' matching

To understand the range of values that some of the unknown parameters can take, the pressure curves obtained with the simulation are compared with some of the experimental ones. An initial check of the model's effectiveness is to see if the values obtained are reasonable numbers for the type of reactor considered. The first parameter that needs to be evaluated is the gas-liquid mass transfer coefficient kla: according to the sensitivity analyses performed in the studies discussed before, it is one of the most influential parameters for the methane production.

Another important parameter is the concentration of microorganisms X, that isn't calculated with the model as the simulation is ran in different conditions without starting each time from the inoculum insertion.

To identify these values two experimental curves at a time are considered and a Matlab code is used to minimize the difference with the

simulated ones. An exact match and a comparison for longer times are difficult to obtain for the following reasons:

- in the reactor the carbon dioxide injections happen less frequently and change the pressure significantly, creating differences in the curves' shape that depend on their timing. In the simulation the gap between the maximum and the minimum CO_2 concentrations accepted is smaller, to have smoother lines that are easier to analyse;
- the simulations curves are almost identical and even small delays in the real curves cause shifts that make the comparison using more than two experimental curves difficult;
- in the simulations only the main processes are considered, while in the real reactor there are more mechanisms that influence the outcome of the experiment. Also small problems with the components can happen and slightly modify the behaviour of the reactor before being detected.

The following images show three comparisons between experimental and simulated curves.

The parameters chosen to obtain them are reported below:

1. **Figure 31**: kla = 8300 $days^{-1}$, X = 0.5 Kg COD/m^3
2. **Figure 32**: kla = 6700 $days^{-1}$, X = 0.5 Kg COD/m^3
3. **Figure 33**: kla = 10500 $days^{-1}$, X = 0.4 Kg COD/m^3

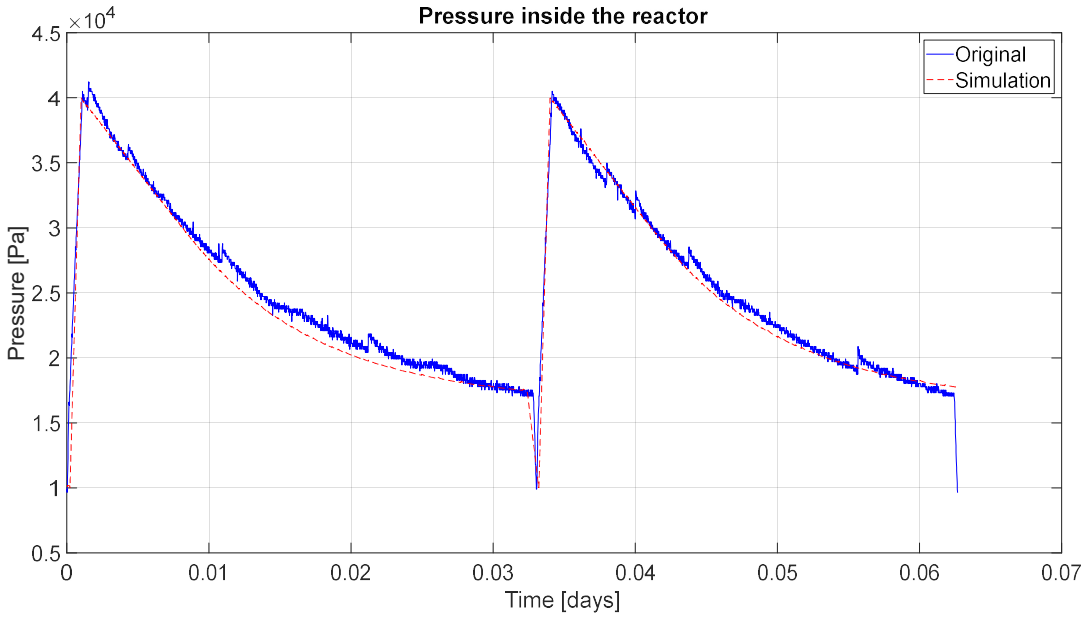

Figure 31 - Simulation curves compared with the experimental ones recorded from 22:34:55 14 March 2025 to 00:05:10 15 March 2025

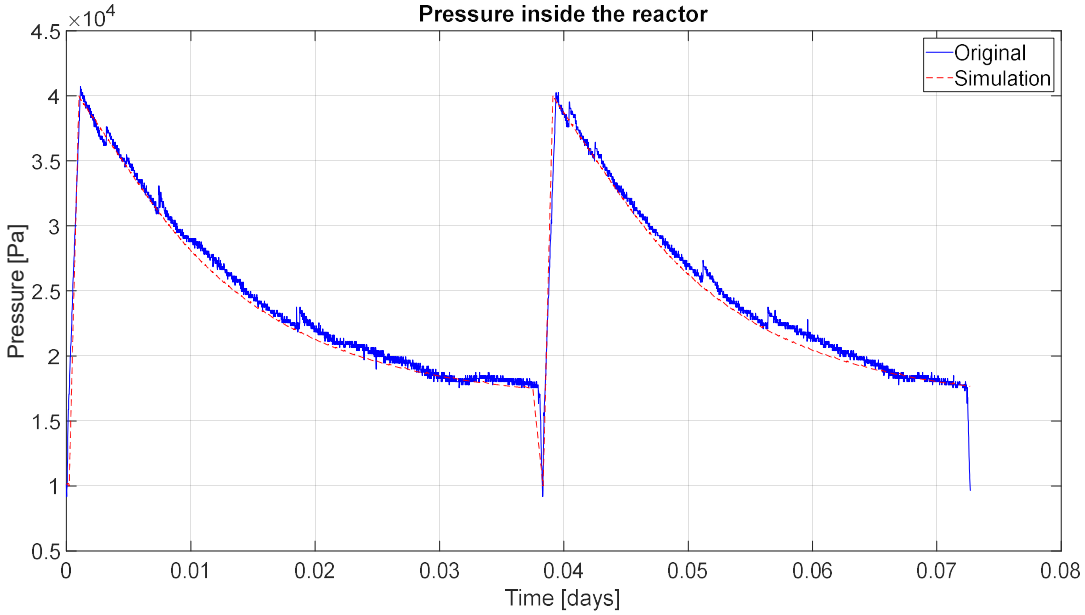

Figure 32 - Simulation curves compared with the experimental ones recorded from 02:42:31 15 March 2025 to 04:27:11 15 March 2025

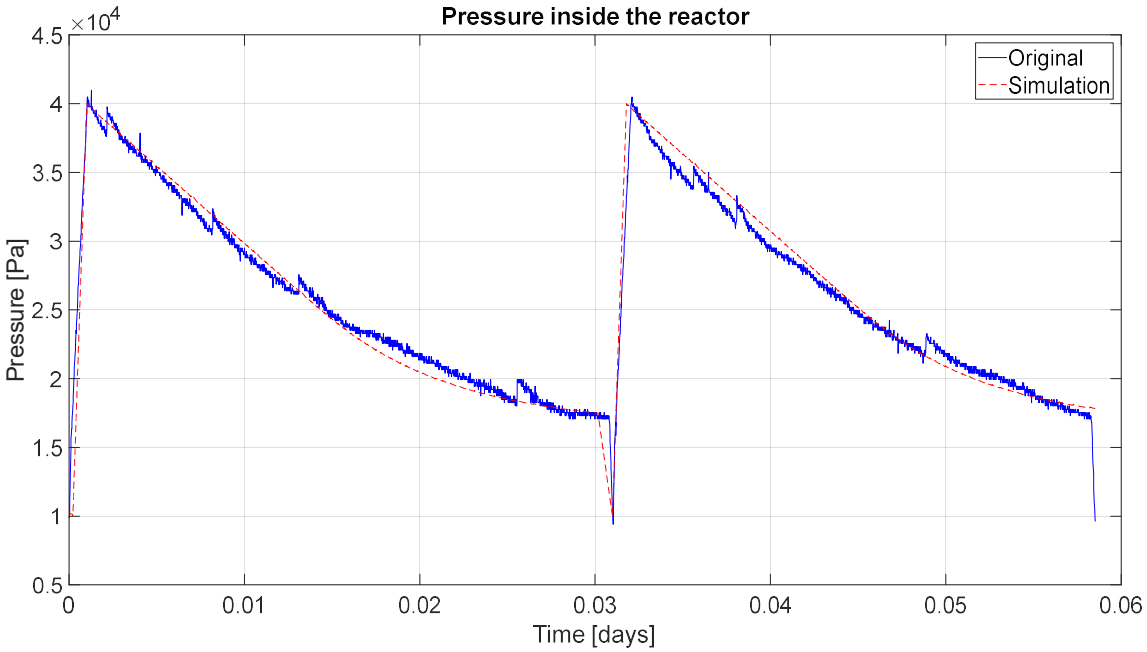

Figure 33 - Simulation curves compared with the experimental ones recorded from 12:53:19 19 March 2025 to 14:17:36 19 March 2025

The values of the gas-liquid mass transfer coefficient are high, remaining between 6700 and 10500 day^{-1}. This is due to the strong mixing mechanism present in the reactor. These numbers are in accordance with the ones reported in literature for laboratory scale CSTR, that go from around 1000 to around 15000 $days^{-1}$ [49].

The concentration of hydrogenotrophic methanogens calculated by the model is around 0.45 kg COD/m^3, which is a reasonable value in the conditions considered.

To verify the accuracy of the model, the MER and methane concentration values found with the model are considered. Working with a kla equal to 9000 $days^{-1}$ and a X of 0.5 kg COD/m^3, that can be considered as representatives of the values obtained from the simulations, the Methane Evolution Rate calculated is equal to 3.32 $Nm^3/(Nm^3 days)$

and the methane presence is equal to 90.7 %. The average data collected from the experimental reactor during the month of March consist in a MER value of 3.59 $Nm^3/(Nm^3days)$ and a methane concentration equal to 92.1 %. The similarity between the experimental values and the ones found on Simulink show that the virtual model is accurate enough to perform studies on the parameters involved and to predict the average production of reactors with different specifics.

4.3.2 Analysis of the impact of the kla and X parameters

Starting from values similar to the ones found for the laboratory reactor, the parameters kla and X are modified and their effect on the curves is studied. As the analyses are executed considering stationary conditions, the concentration of microorganisms X is kept constant in time. In the diagram, the impact of higher kla values is shown.

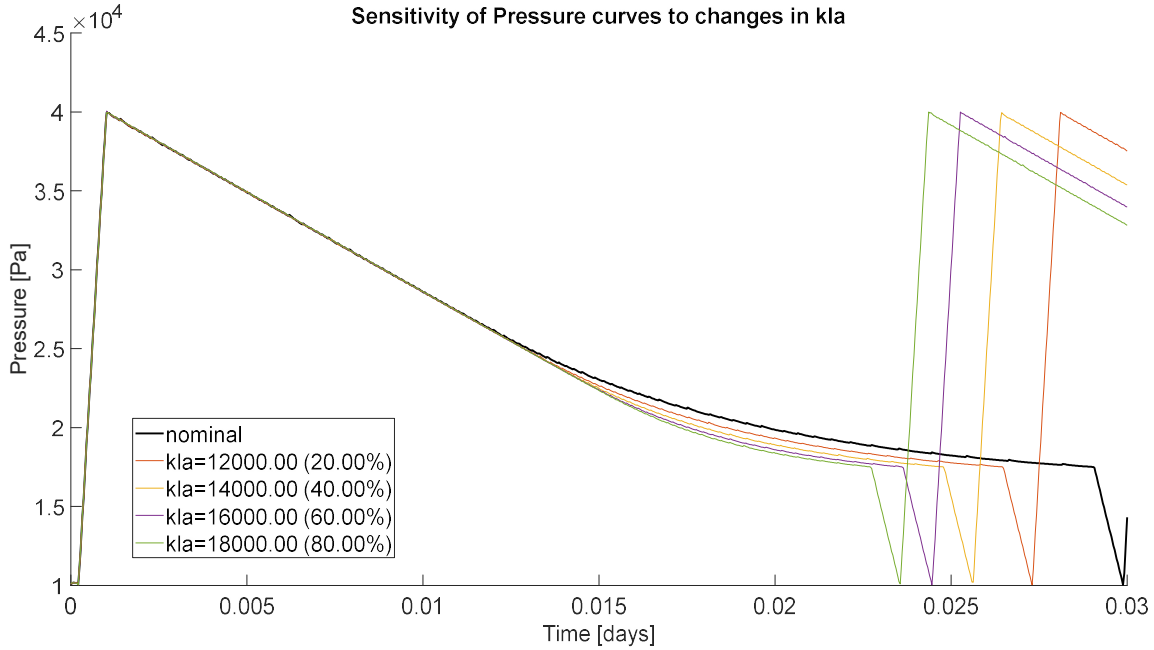

Figure 34 - Diagram showing how the pressure curves change with the parameter kla

It can be seen that the cycle becomes faster as the kla values increase. It's important to observe how the shape of the curve changes: in the first part the curves are the same while later the lower the kla value the sooner the pressure deviates from the straight line. In the beginning the methane production speed is constant, because the hydrogen concentration in the liquid is high enough, while later the hydrogen presence decreases and causes a partial inhibition of the process.

When the gas-liquid mass transfer coefficient is higher, the hydrogen concentration remains high enough for a longer period. This phenomenon is regulated by the term $X/(k_{s,H2} + X)$, whose trend is shown in the diagram below.

It's clear that when the kla values are higher the value of this term remains equal to one for more time: this means that the hydrogen concentration is sufficient for the microorganisms to digest at full speed.

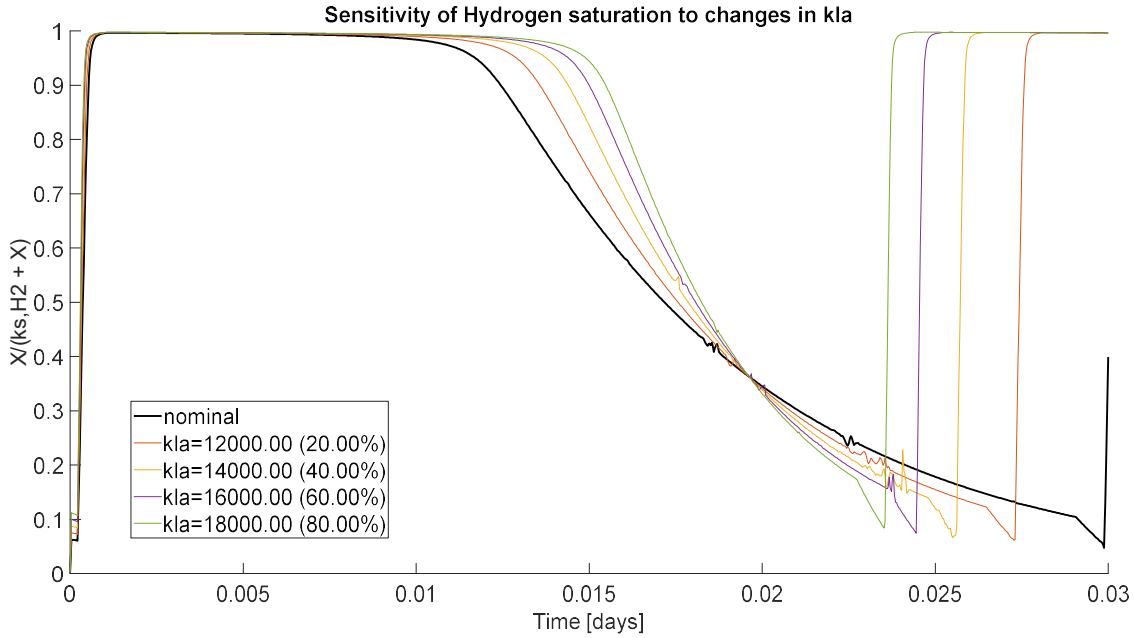

Figure 35 - Diagram showing how the term $X/(k_{s,H2} + X)$ is affected by the parameter kla

The same behaviour can be seen for the curves plotted with kla values lower than the experimental one.

As visible in the diagram below, for kla values lower than 2000 $days^{-1}$ the first linear part is not present as the hydrogen concentration is never high enough to generate it.

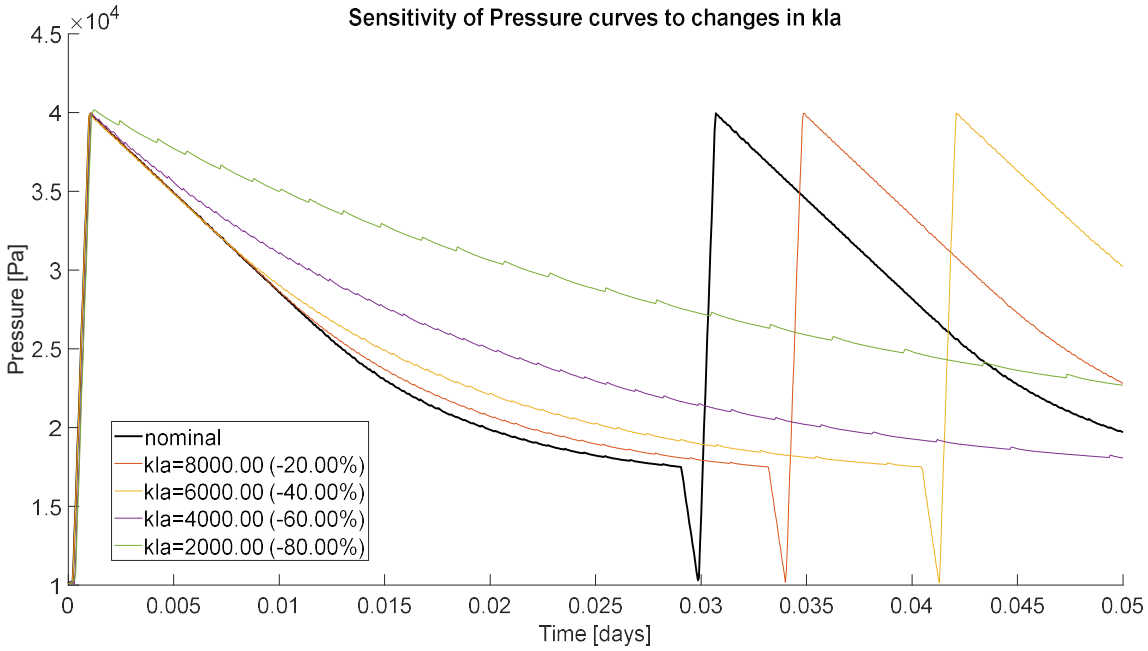

Figure 36 - Diagram showing how the pressure curves change with the parameter kla

The MER and the methane presence at the outlet are the most significant parameters to understand how well a biomethanation reactor works and it's important to study how they are influenced by the kla.

The images below show this relationship.

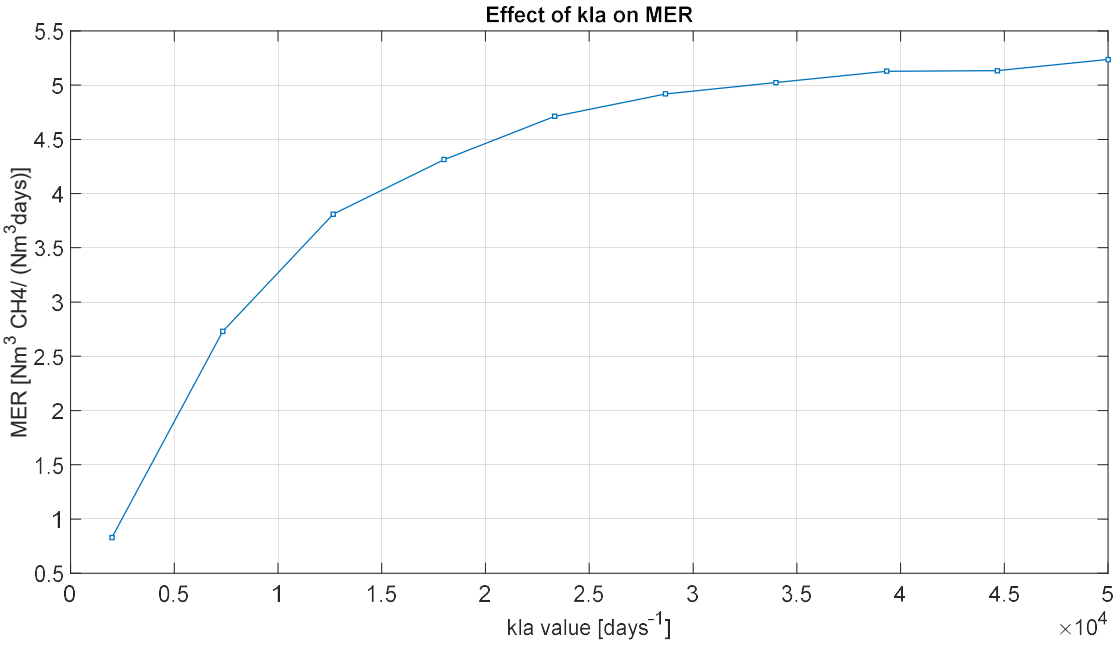

Figure 37: diagram showing the trend of the MER as the kla changes

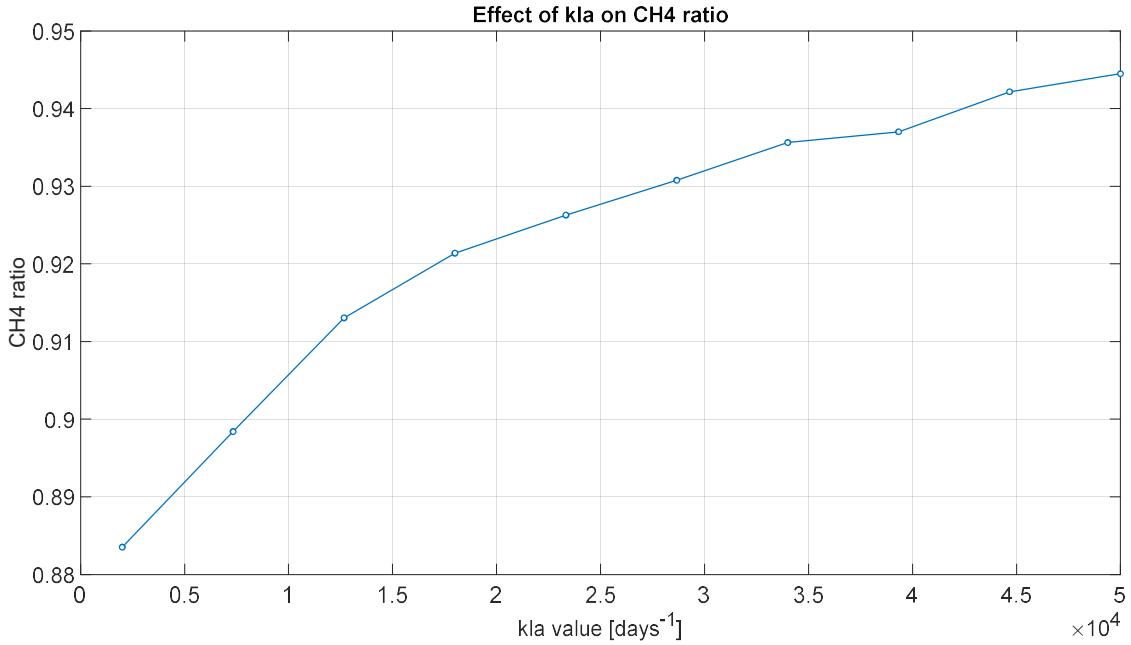

Figure 38 - Diagram showing the trend of the methane concentration as the kla changes

It can be seen how the values of the parameters improve as the gas-liquid mass transfer coefficient increases: this is the reason why the different reactor configurations are built to maximize this effect. Once the kla becomes bigger than a certain value, the improvements become smaller. This is because the pressure curves become almost entirely straight lines and so the speed is limited by the concentration of microorganisms. For a concentration of 0.4 kg COD/m^3 of microorganisms, this value is around 30000 day^{-1}.

The same analysis is now carried out modifying the concentration of hydrogenotrophic methanogens, X.

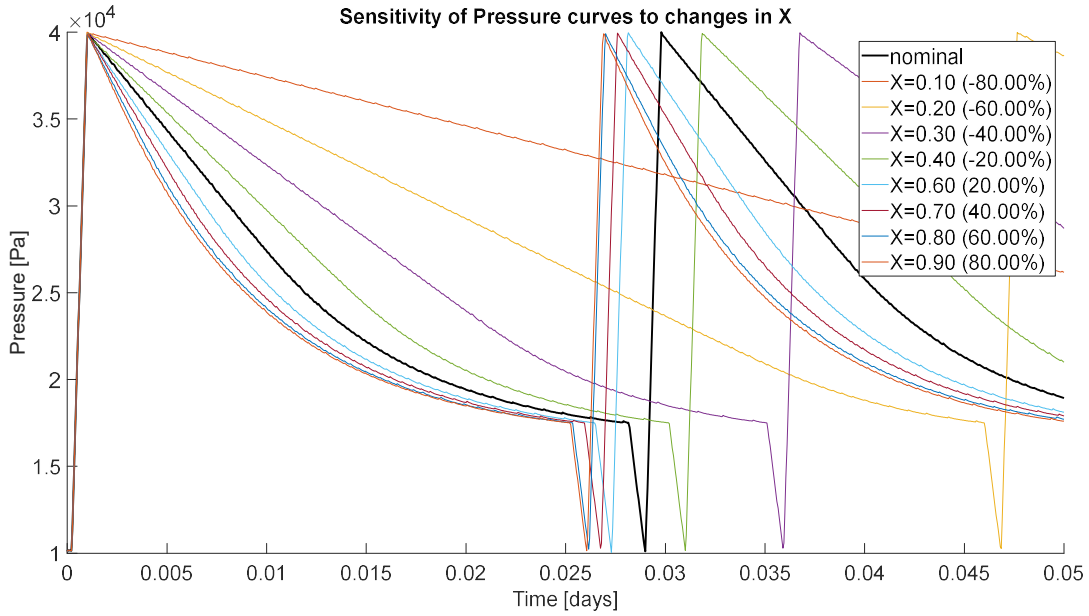

Figure 39 - Diagram showing how the pressure curves change with the parameter X

As the concentration of microorganisms increases, the methanation's speed increases too. At higher concentrations the impact of the variations is smaller because of the inhibition related to the scarcity of hydrogen. At low concentrations the hydrogen remains enough for all the

microorganisms to digest at full speed and the curves are linear for the majority of the time.

Also in this case this phenomenon can be observed looking at the variation of the term $X/(k_{s,H2} + X)$. When the X is low, the term remains equal to one for longer times, as the concentration of hydrogen is not limiting the digestion's speed.

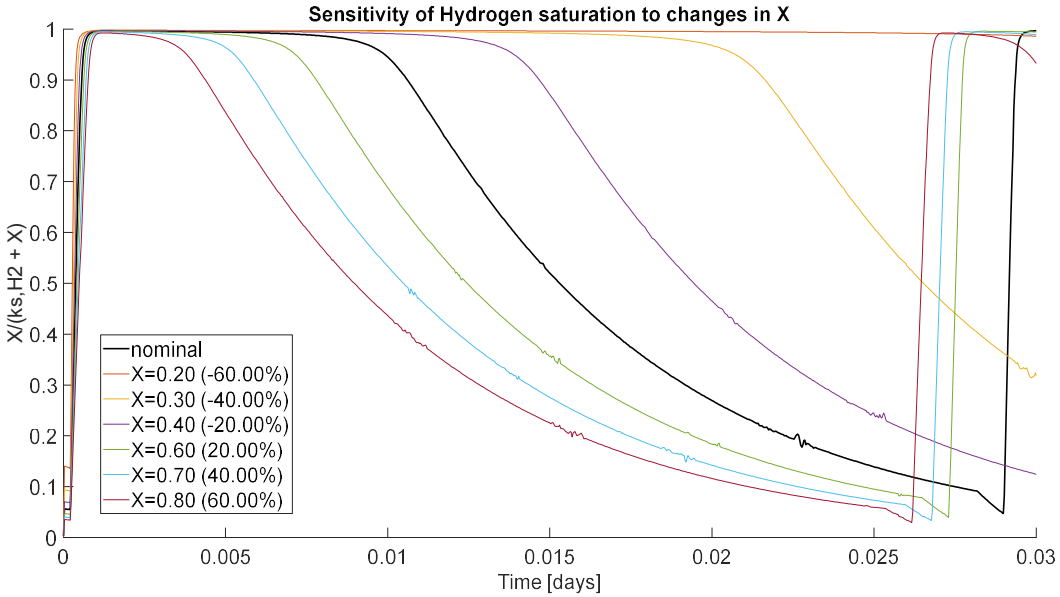

Figure 40 - Diagram showing how the term $X/(k_{s,H2} + X)$ is affected by the parameter X

For higher concentration of methanogens, the issue becomes that the hydrogen is not enough and the process is strongly limited by the term analysed before, as it can be seen in the following diagram.

For this reason, the production doesn't increase much if there isn't an increase also of the kla parameter or of the pressure inside the reactor.

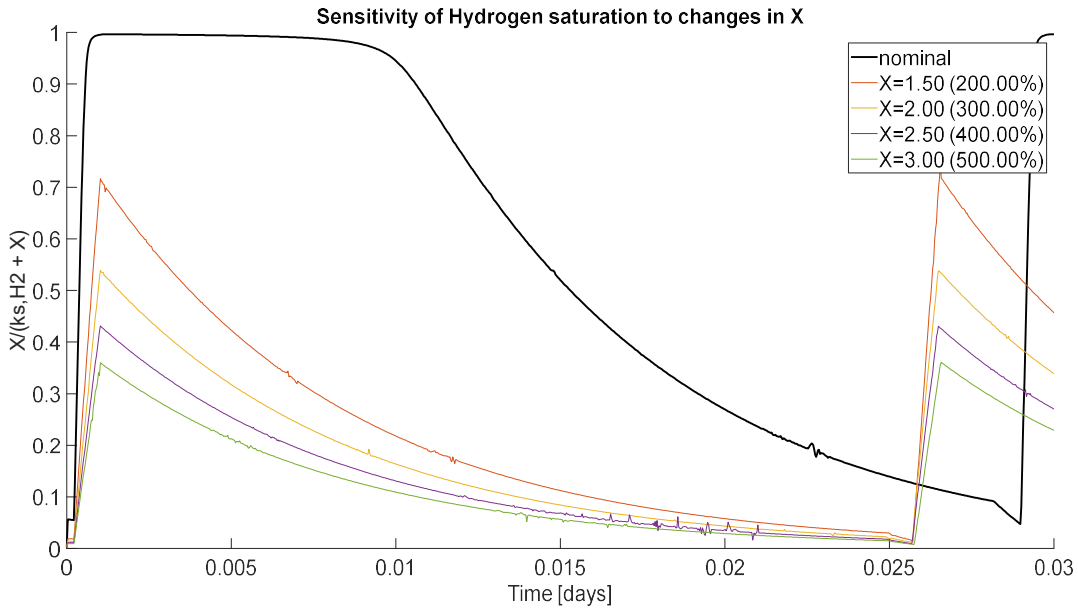

Figure 41 - Diagram showing how the term $X/(k_{s,H2} + X)$ is affected by the parameter X

Let's now consider the how the MER and methane presence values can improve when the concentration of microorganisms increases.

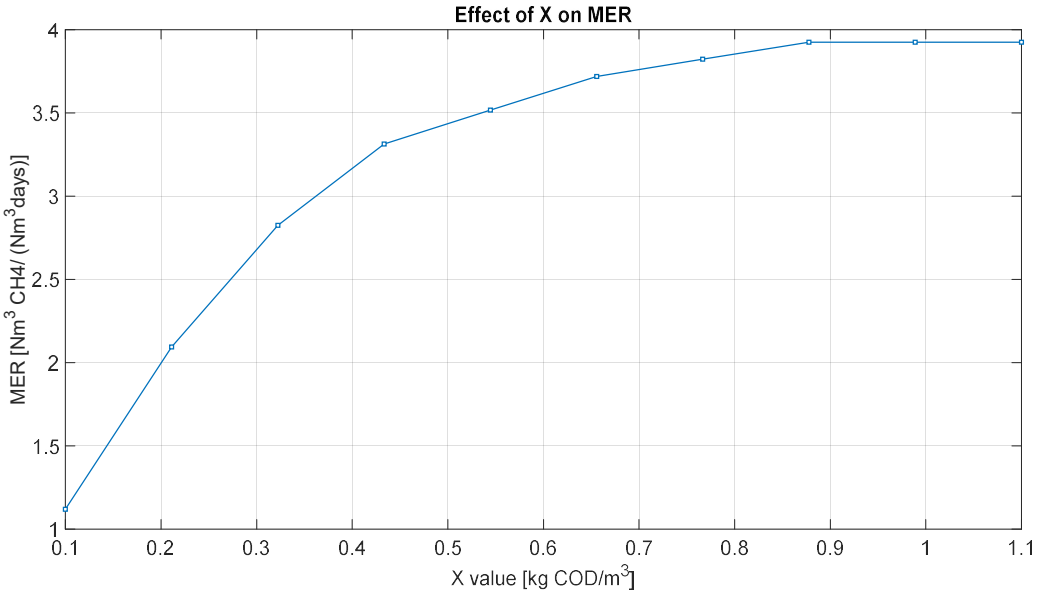

Figure 42 - Diagram showing the trend of the MER as the X changes

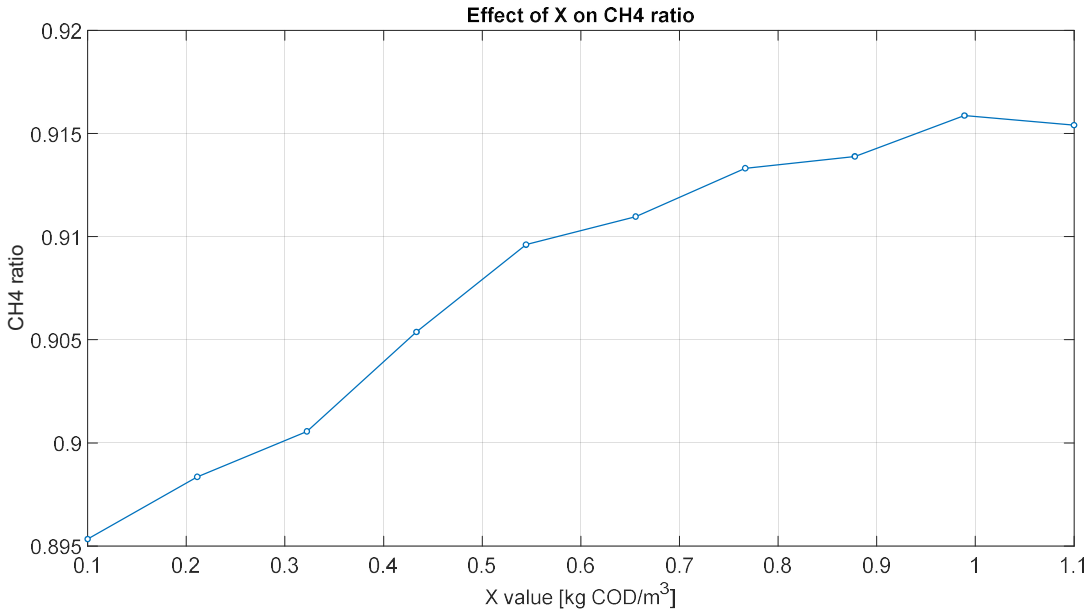

Figure 43 - Diagram showing the trend of the methane concentration as the X changes

Looking at Figure 42, it's clear that after approximately a value of 0.6 kg COD/m^3 the methane production doesn't improve anymore, because of the inhibition caused by the scarcity of hydrogen. The ratio of CH_4 at the outlet instead keeps improving, but slowly and without reaching the values obtained increasing the kla.

After having analysed the impact of these parameters separately, it's necessary to see how the system behaves when both of them are different from the original values.

From the diagram below it's clear that as the concentration of methanogens increase, the value of the kla reached before the flattening of the curve becomes higher.

This means that when the concentration of microorganisms is high, an increase in the kla value still gives a solid improvement even if it's already in the high value range.

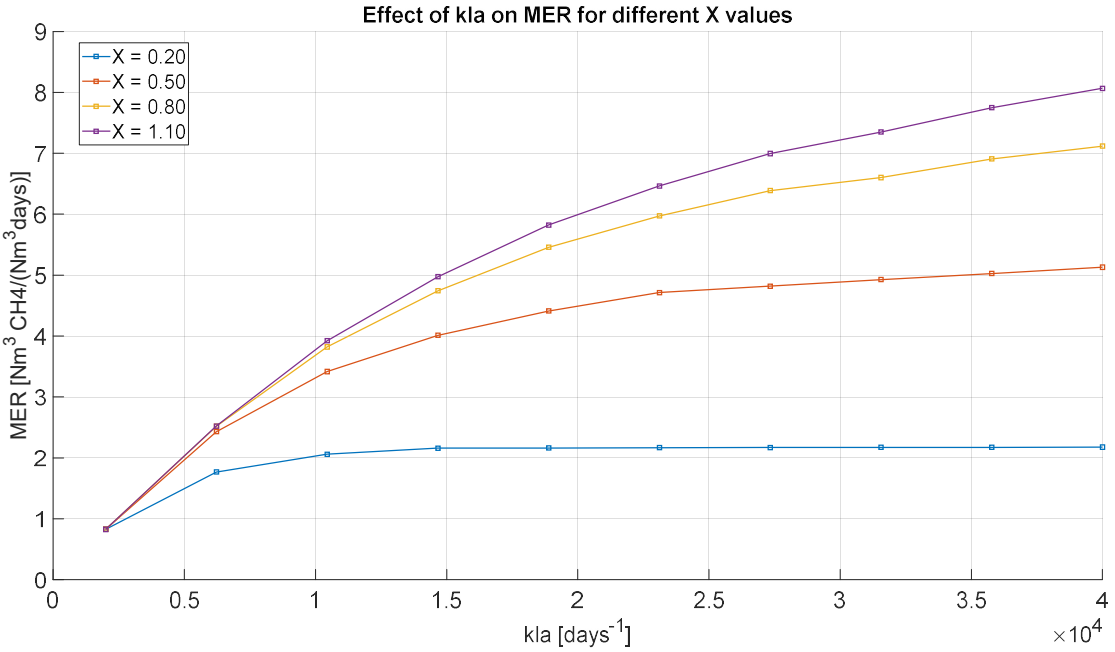

Figure 44 - Diagram showing the trend of the MER as the kla changes, for different values of X

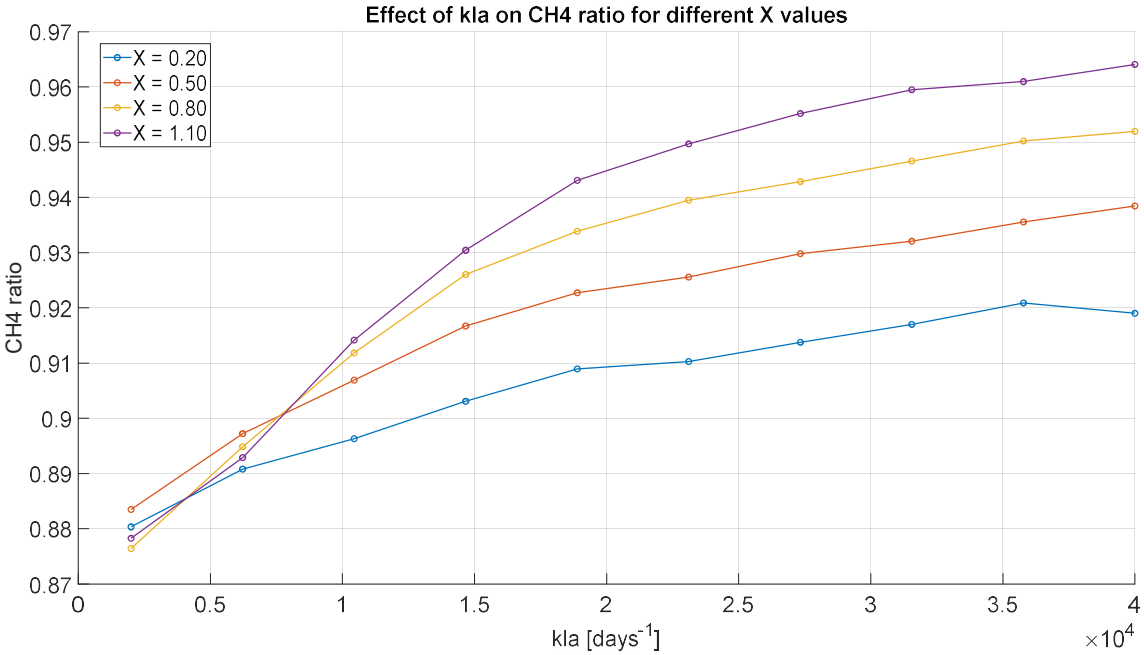

Figure 45 - Diagram showing the trend of the methane concentration as the kla changes, for different values of X

4.3.3 Analysis of the impact of the pressure

The pressure in the reactor is an important parameter as it influences the concentration of hydrogen present in the liquid phase and so the speed of the entire process. When the pressure is higher, the concentration of H_2 at the liquid surface increases and, according to Fick's law of diffusion, the gas-liquid mass transfer does the same.

The diagram below considers small changes in the minimum pressure reached during the cycle, Poffset, while the pressure gaps for charge and discharge are maintained constant. The pressure values are always expressed as a difference with respect to the atmospheric one.

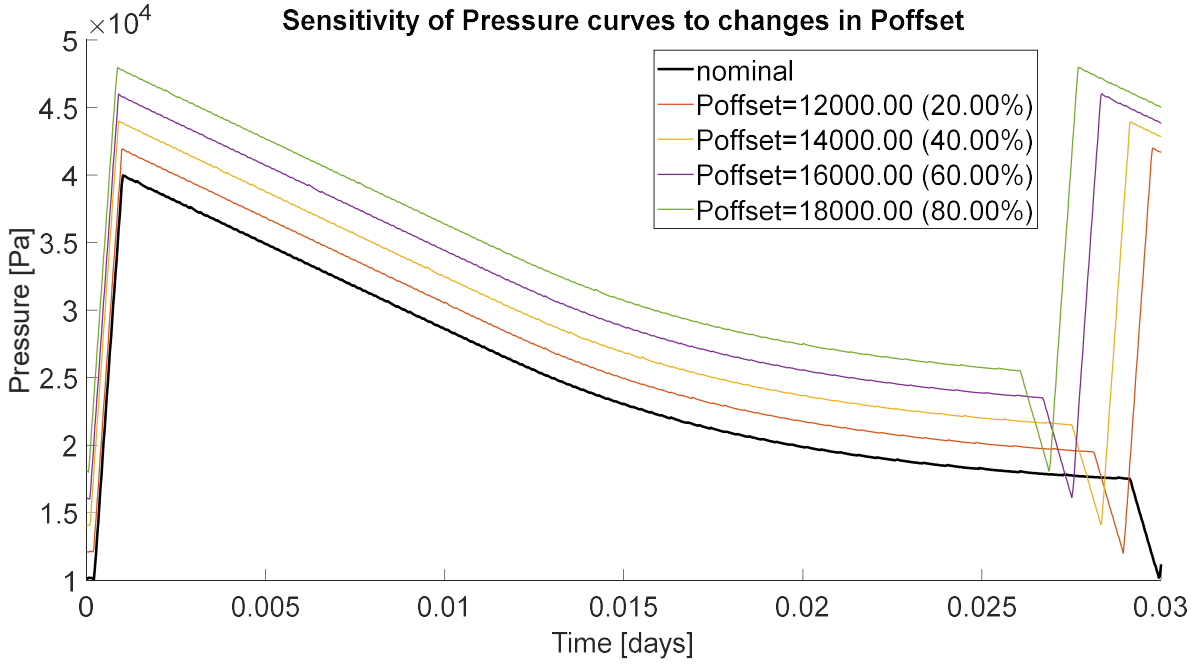

Figure 46: diagram showing how the pressure curves change with the minimum internal pressure

As the mass transfer from gas to liquid improves, the production cycle becomes faster, especially in the last part when there is scarcity of hydrogen in the headspace.

The kla parameter of the laboratory reactor is around 10000 $days^{-1}$ and, because of technical limitations, even modifying the reactor configuration it can't be increased more than around eight times this value. On the other hand, the internal pressure can be increased a lot more, as the maximum pressure reached in the laboratory reactor is equal to only 400 mbar and in more complex reactors it can be of 8-10 bar. The effect that high pressure has on the production is shown in the following diagrams. Different curves related to different microorganisms' concentrations are plotted to ensure that the process is not inhibited by the number of methanogens.

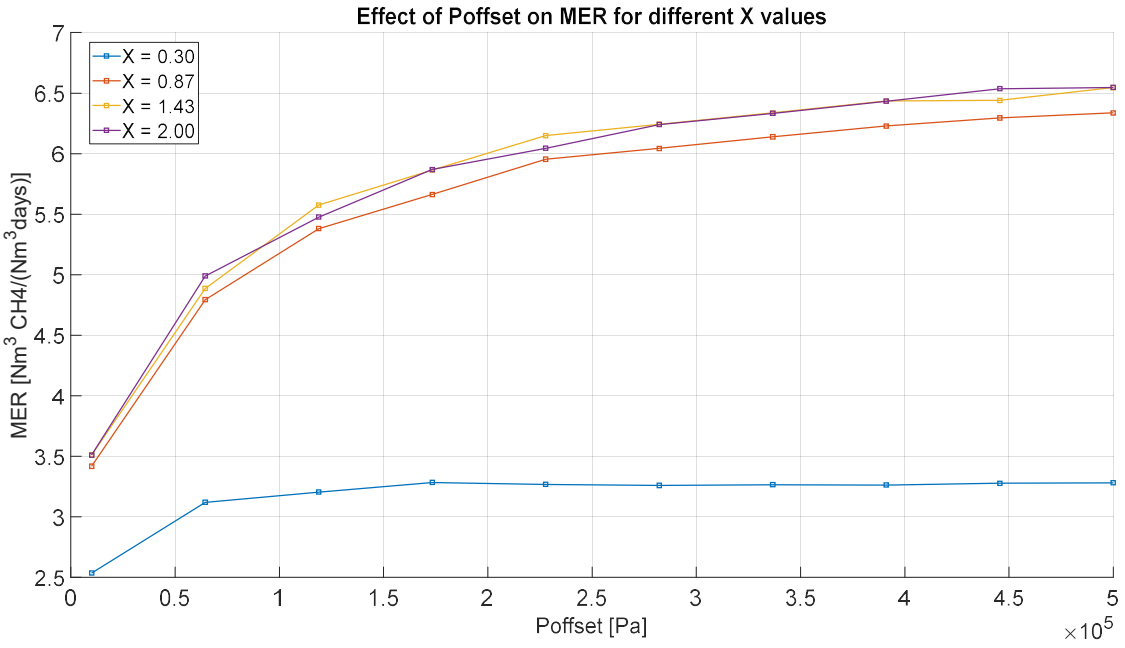

Figure 47 - Diagram showing the trend of the MER as the minimum internal pressure changes, for different values of X

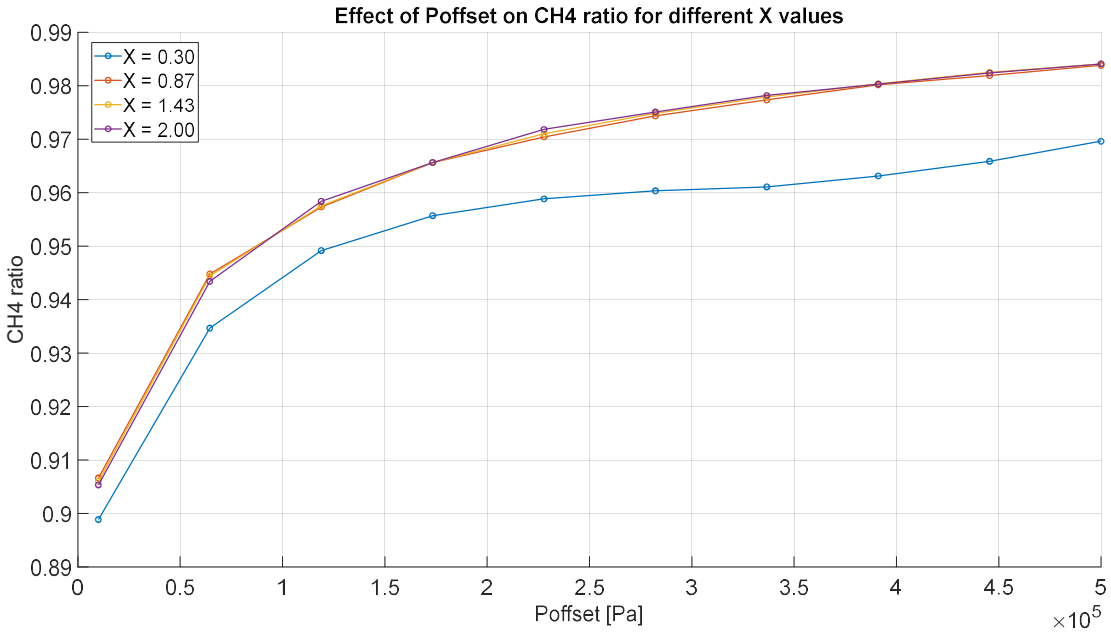

Figure 48 - Diagram showing the trend of the methane concentration as the minimum internal pressure changes, for different values of X

It's immediately clear that a too low concentration of microorganisms strongly limits the potential production. Even with higher X values however, the MER doesn't increase as expected: for pressure more than ten times higher, only MER values of around 6 $Nm^3/(Nm^3days)$ are reached. This can be explained looking at the ratio of methane in the outlet gas, as high values are obtained and cause low hydrogen concentrations even at high pressure.

This situation is not optimal from a production point of view, as in the vast majority of the cases it's not necessary to have a methane concentration higher than around 98 %. To solve this issue, the gap between the maximum pressure and the discharge pressure has to be modified: until now the gap was chosen to theoretically remove a number of moles equal to the ones of methane produced using all the hydrogen

injected in a cycle, but less methane has to be removed to keep the H_2 concentration in the headspace high enough.

The following diagrams show variations of the gap between the minimum pressure and the discharge pressure, called MinGap in the model. The MER and CH_4 ratio in the outlet gas are calculated for different concentrations of methanogens and in the cases of a minimum pressure of 3, 5 and 8 bar.

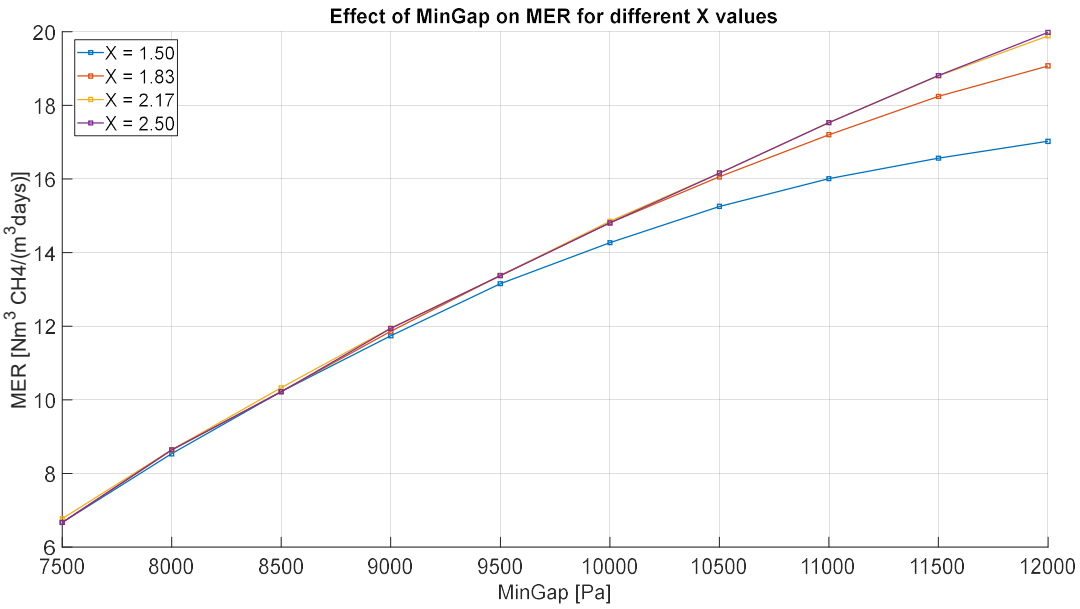

Figure 49 - Diagram showing the trend of the MER as the discharge pressure changes, for different values of X and with a minimum pressure of 3 bar

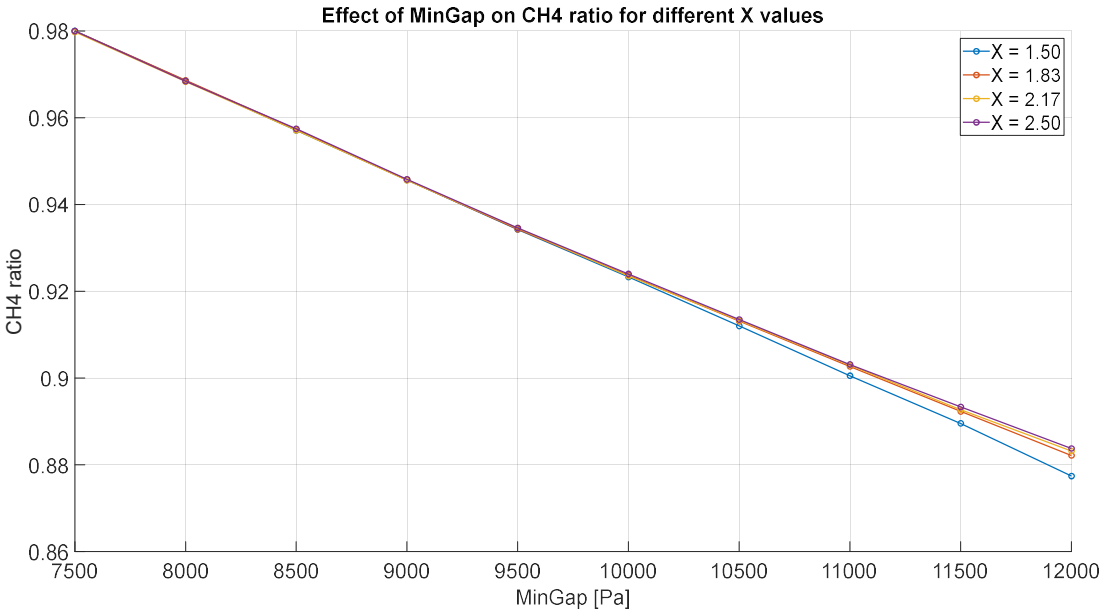

Figure 50 - Diagram showing the trend of the methane concentration as the discharge pressure changes, for different values of X and with a minimum pressure of 3 bar

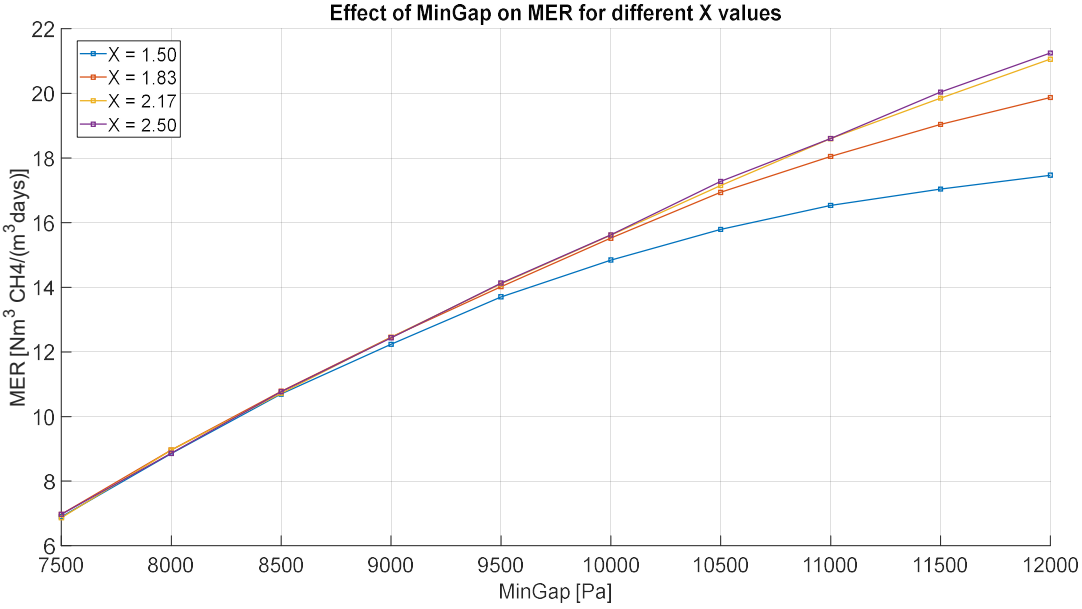

Figure 51 - Diagram showing the trend of the MER as the discharge pressure changes, for different values of X and with a minimum pressure of 5 bar

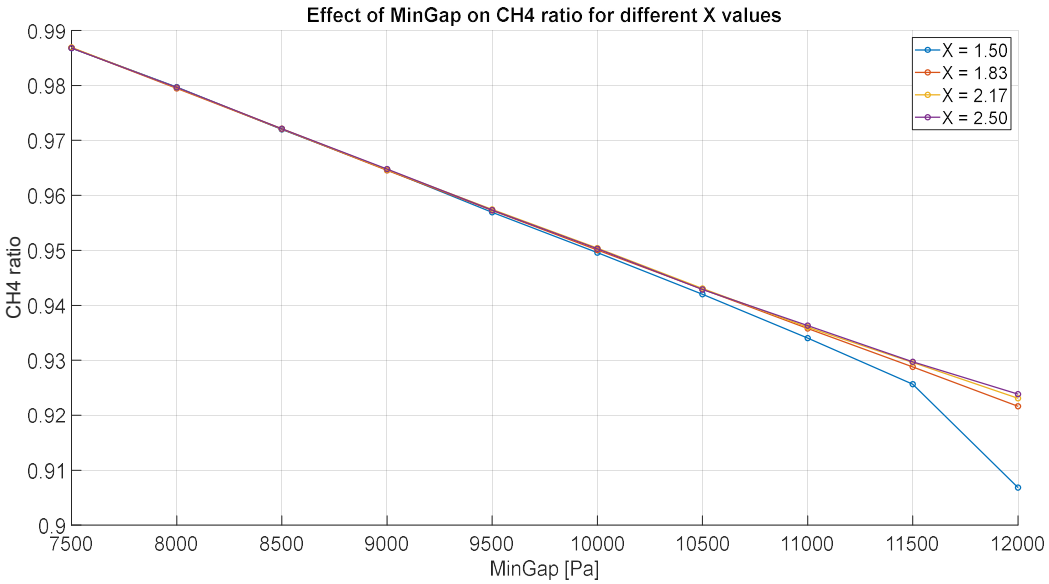

Figure 52 - Diagram showing the trend of the methane concentration as the discharge pressure changes, for different values of X and with a minimum pressure of 5 bar

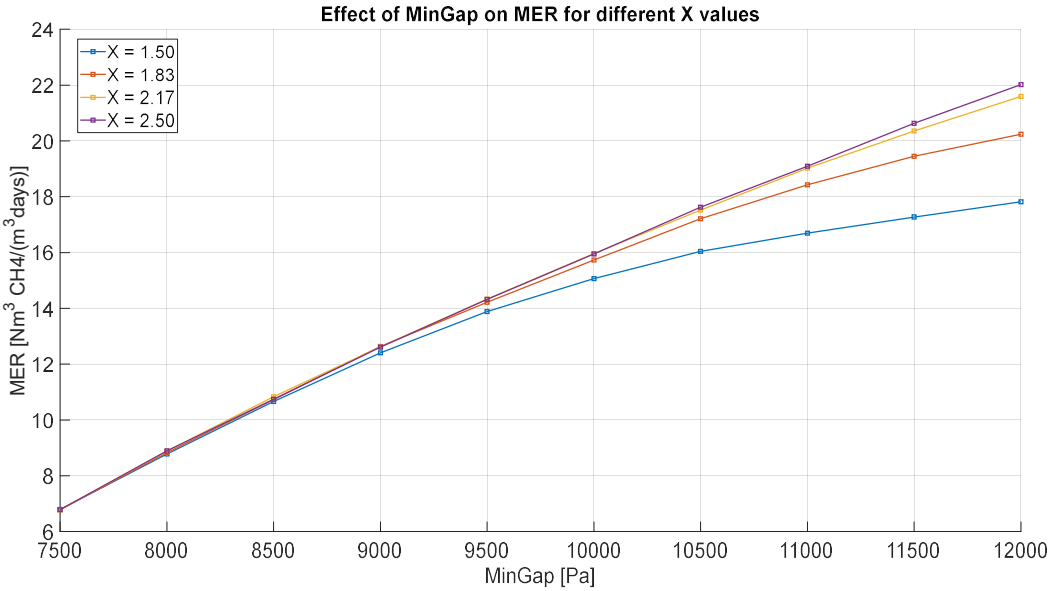

Figure 53 - Diagram showing the trend of the MER as the discharge pressure changes, for different values of X and with a minimum pressure of 8 bar

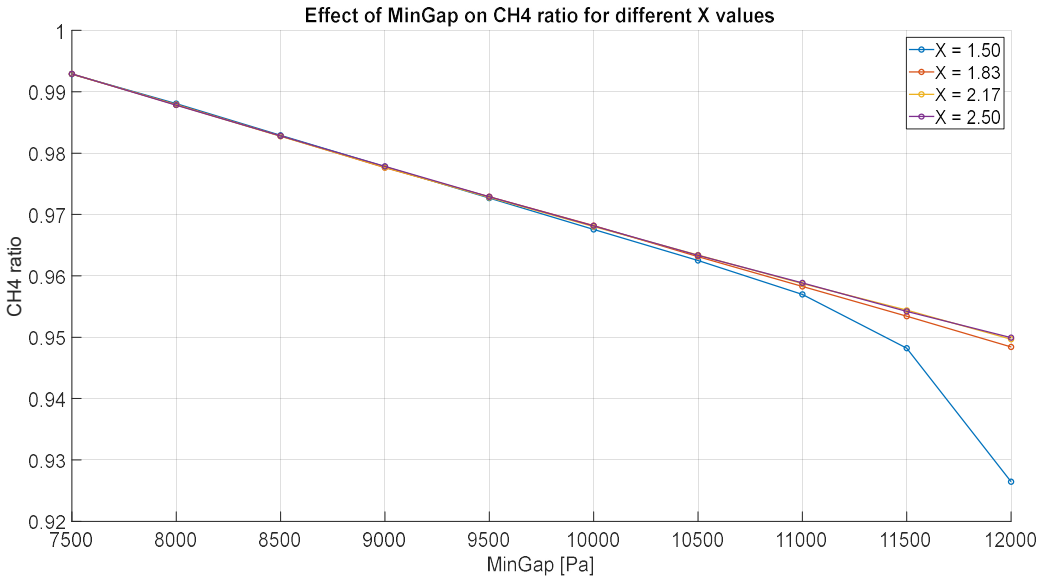

Figure 54 - Diagram showing the trend of the methane concentration as the discharge pressure changes, for different values of X and with a minimum pressure of 8 bar

5. Conclusions

From the results of the simulations, the impact that the different parameters have on the pressure cycle and on the methane production is analysed.

The first parameter studied is the gas-liquid mass transfer coefficient kla. In accordance with many previous analyses, it's observed that it has a major influence on the speed of the process and that it enables the microorganisms to digest at full speed even at lower hydrogen concentrations.

It's then analysed the influence of the concentration of hydrogenotrophic methanogens. A higher number of microorganisms doesn't cause a big improvement in the process if the kla and pressure parameters remain constant, but it's vital to be able to exploit higher values of these two parameters.

Working at the low pressure values of the laboratory reactor, some of the results achievable with reasonable kla values and with a sufficiently high X are reported in the table below.

kla [$days^{-1}$]	CH_4 ratio [%]	MER [$Nm^3/(Nm^3 days)$]
10000	91.5	3.8
20000	94.5	6.1
30000	95.8	7.2
40000	96.3	8.1

From the analysis, it emerges how the internal pressure is a key parameter, especially because of the possibility to increase it in a consistent way with respect to the laboratory conditions.

It's observed that, keeping the gap between the maximum pressure and the discharge pressure constant, the MER values don't increase as much as expected, mainly because of the high concentration of methane reached in the headspace.

To understand the real potential of working at high pressure, the discharge point is shifted and scenarios with different compromises between the methane concentration and the MER are obtained. In the table below the results are compared, considering pressure values of 3,5 and 8 bar.

As the production rate increases, it's important to take in consideration the heat generated during the process. The methanation reaction has a negative enthalpy change and, for every mole of methane produced, 165.01 kJ of heat are released in standard conditions. In the laboratory reactor, this isn't a crucial detail because of the small quantity produced, but in big industrial systems it's important to exploit this energy to maintain the temperature and eventually use it in other processes.

In the case of thermophilic or hyper-thermophilic conditions, the temperature would be higher and so also the exergy of the heat generated would be better. In the table below the heat produced daily is reported.

Minimum pressure [bar]	CH_4 ratio [%]	MER [$Nm^3/(Nm^3 days)$]	Heat generated [KJ/day]
3	95	10.9	114.5
	98	6.7	69.7
5	95	15.6	162.3
	98	9.1	94.7
8	95	22.1	229.0
	98	11.8	122.8

For what concerns future applications, this model can be useful to predict the performance of different ex-situ reactors and determine which modifications are worthy of being implemented.

In the laboratory where the system discussed in this work was studied, a new reactor is being set up. It can reach an internal pressure of 8 bar, and it has a total volume of 14 L.

The goal is to use the virtual model to try to predict its production and then see if the results are valid also in case of larger systems.

LIST OF FIGURES

REFERENCES

[1] U. S. Energy Information, «International Energy Outlook 2023».

[2] International Energy Agency, «World Energy Outlook 2024».

[3] International Energy Agency, «Net Zero by 2050 Report,» 2021.

[4] International Energy Agency, 2022.

[5] International Energy Agency, «More of a good thing – is surplus renewable electricity an opportunity for early decarbonisation?,» 2019.

[6] European Union, «Renewable Energy Directive II,» 2009.

[7] European Union, «Renewable Energy Directive III,» 2023.

[8] T. Schaaf, J. Grünig, M. R. Schuster, T. Rothenfluh e A. Orth, «Methanation of CO2 - storage of renewable energy in a gas distribution system,» *Energy, Sustainability and Society,* vol. 4, 2014.

[9] International Energy Agency, «Global Hydrogen Review 2024».

[10] S. S. Kumar e H. Lim, «An overview of water electrolysis technologies for green hydrogen production,» *Energy Reports,* vol. 8, pp. 13793-13813, 2022.

[11] M. Götz, J. Lefebvre, F. Mörs, A. M. Koch, F. Graf, S. Bajohr, R. Reimert e T. Kolb, «Renewable Power-to-Gas: A technological and economic review,» *Renewable Energy,* vol. 85, pp. 1371-1390, 2016.

[12] W. J., Carbon Capture, Springer Science & Business Media, 2012.

[13] E. Hanson, C. Nwakile e V. O. Hammed, «Carbon capture, utilization, and storage (CCUS) technologies: Evaluating the effectiveness of advanced CCUS solutions for reducing CO2 emissions,» *Results in Surfaces and Interfaces,* vol. 18, 2025.

[14] A. P. Raganati F., «CO2 Post-combustion Capture: A Critical Review of Current Technologies and Future Directions,» *Energy & Fuels,* vol. 38, n. 15, pp. 13858-13905.

[15] P. Basu, Biomass Gasification and Pyrolysis - Practical design, Academic Press, 2010.

[16] Z. Feng e X. He, «Current Status and Analysis of Natural Gas Pipeline Hydrogen Blending and Transportation Development,» *International Journal of Electric Power and Energy Studies,* vol. 2, n. 3, 2024.

[17] A. Ekhtiari, D. Flynn e E. Syron, «Green Hydrogen Blends with Natural Gas and Its Impact on the Gas Network.,» *Hydrogen,* vol. 3, n. 4, pp. 402-417, 2022.

[18] B. Lecker, L. Illi, A. Lemmer e H. Oechsner, «Biological hydrogen methanation – A review,» *Bioresource Technology, Volume 245, Part A,* pp. 1220-1228, 2017.

[19] J. B. van Lier, N. Mahmoud e G. Zeeman, «16: Anaerobic wastewater treatment,» in *Biological Wastewater Treatment: Principles, Modelling and Design*, IWA Publishing, 2023, pp. 401-441.

[20] F. B. Sarmiento, J. A. Leigh e W. B. Whitman, «Chapter three - Genetic Systems for Hydrogenotrophic Methanogens,» in *Methods in Enzymology*, vol. 494, Academic Press, 2011, pp. 43-73.

[21] S. Åström, «The Effect of Pyrolysis Water on Different Levels of a Reactor for Biological Syngas Methanation,» 2024.

[22] E. Cazier, E. Trably, J. Steyer e R. Escudie, «Biomass hydrolysis inhibition at high hydrogen partial pressure in solid-state anaerobic digestion,» *Bioresource Technology,* vol. 190, pp. 106-113, 2015.

[23] P. Tsapekos, M. Alvarado-Morales e I. Angelidaki, «H2 competition between homoacetogenic bacteria and methanogenic archaea during,» *Journal of Environmental Chemical Engineering,* Vol. %1 di %210, Issue 2, 2022.

[24] M. Fachal-Suárez, S. Krishnan, S. Chaiprapat, D. González e D. Gabriel, «An overview of biomethanation and the use of membrane technologies as a candidate to overcome H2 mass transfer limitations,» *Biotechnology Advances,* vol. 77, 2024.

[25] A. Chatzis, P. Gkotsis e A. Zouboulis, «Biological methanation (BM): A state-of-the-art review on recent research advancements and practical implementation in full-scale BM units,» *Energy Conversion and Management,* vol. 314, 2024.

[26] M. Jensen, L. Ottosen e M. Kofoed, «H2 gas-liquid mass transfer: A key element in biological Power-to-Gas methanation,» *Renewable and Sustainable Energy Reviews,* vol. 147, 2021.

[27] D. Pokorna, Z. Varga, D. Andreides e J. Zabranska, «Adaptation of anaerobic culture to bioconversion of carbon dioxide with hydrogen to biomethane,» *Renewable Energy,* vol. 142, pp. 167-172, 2019.

[28] X. Zhu, L. Chen, Y. Chen, Q. Cao, X. Liu e D. Li, «Differences of methanogenesis between mesophilic and thermophilic in situ biogas-upgrading systems by hydrogen addition,» *J Ind Microbiol Biotechnol,* pp. 1569-1581, 2019.

[29] D. G. Mulat, F. Mosbæk, A. J. Ward, D. Polag, M. Greule, F. Keppler, J. L. Nielsen e A. Feilberg, «Exogenous addition of H2 for an in situ biogas upgrading through biological reduction of carbon dioxide into methane,» *Waste Management,* vol. 68, pp. 146-156, 2017.

[30] R. Wahid, D. G. Mulat, J. C. Gaby e S. J. Horn, «Effects of H2:CO2 ratio and H2 supply fluctuation on methane content and microbial community composition during in-situ biological biogas upgrading,» *Biotechnol Biofuels,* vol. 12, 2019.

[31] A. Grimalt Alemany, I. V. Skiadas e H. N. Gavala, «Syngas biomethanation: state-of-the-art review and perspectives,» *Biofuels, Bioproducts and Biorefining,* vol. 12, p. 139–158, 2018.

[32] Electrochaea GmbH, «electrochaea,» [Online]. Available: https://www.electrochaea.com/. [Consultato il giorno 12 11 2025].

[33] InnoEnergy, «Decarbonising industry, Enosis,» [Online]. Available: https://innoenergy.com/portfolio/enosis.com.

[34] Kanadevia Inova, «Kanadevia Inova Power to Gas,» [Online]. Available: https://www.kanadevia-inova.com/it/renewable-gas/power-to-gas/.

[35] G. Luo e I. Angelidaki, «Integrated biogas upgrading and hydrogen utilization in an anaerobic reactor containing enriched hydrogenotrophic methanogenic culture,» *Biotechnology and Bioengineering,* Vol. %1 di %2109, Issue 11, 2012.

[36] M. Voelklein, D. Rusmanis e J. Murphy, «Biological methanation: Strategies for in-situ and ex-situ upgrading in anaerobic digestion,» *Applied Energy,* vol. 235, pp. 1061-1071, 2019.

[37] L. Laguillaumie, Y. Rafrafi, E. Moya-Leclair, D. Delagnes, S. Dubos, M. Spérandio, E. Paul e C. Dumas, «Stability of ex situ biological methanation of H2/CO2 with a mixed microbial culture in a pilot scale bubble column reactor,» *Bioresource Technology,* vol. 34, 2022.

[38] L. Rachbauer, G. Voitl, G. Bochmann e W. Fuchs, «Biological biogas upgrading capacity of a hydrogenotrophic community in a trickle-bed reactor,» *Applied Energy,* vol. 180, pp. 483-490, 2016.

[39] P. Tsapekos, L. Treu, S. Campanaro, V. B. Centurion, X. Zhu, M. Peprah, Z. Zhang, P. G. Kougias e I. Angelidaki, «Pilot-scale biomethanation in a trickle bed reactor: Process performance and microbiome functional reconstruction,» *Energy Conversion and Management,* vol. 244, 2021.

[40] D. Batstone, J. Keller, I. Angelidaki, S. Kalyuzhnyi, S. Pavlostathis, A. Rozzi, W. Sanders, H. Siegrist e V. Vavilin, «The IWA Anaerobic Digestion Model No 1 (ADM1),» *Water Science and Technology,* vol. 45, n. 10, p. 65–73, 2002.

[41] Y. Shang, B. R. Johnson, R. Sieger e R. Forbes, «Application of the IWA Anaerobic Digestion Model (ADM1) for simulating full-scale anaerobic sewage sludge digestion,» *Water science and technology,* vol. 52, pp. 487-492, 2005.

[42] A. Santus, V. Corbellini, M. Trionfini, F. Malpei e G. Ferretti, «Modelling and Parameter Identification of Ex-Situ Biological Biogas Upgrading,» *IFAC-PapersOnLine,* vol. 55, n. 20, pp. 624-629, 2022.

[43] I. Bassani, P. Kougias, L. Treu, H. Porté, S. Campanaro e I. Angelidaki, «Optimization of hydrogen dispersion in thermophilic up-flow reactors for ex situ biogas upgrading,» *Bioresource Technology,* vol. 234, pp. 310-319, 2017.

[44] G. Lovato, M. Alvarado-Morales, A. Kovalovszki, M. Peprah, P. Kougias, J. A. D. Rodrigues e I. Angelidaki, «In-situ biogas upgrading process: modeling and simulations aspects,» *Bioresource Technology,* vol. 245(Part A), pp. 332-341, 2017.

[45] J. Zambrano, I. Krustok, E. Nehrenheim e B. Carlsson, «A simple model for algae-bacteria interaction in photo-bioreactors,» *Algal Research,* vol. 19, pp. 155-161, 2016.

[46] R. Sander, «Compilation of Henry's law constants (Version 4.0) for water as solvent,» *Atmospheric Chemistry and Physics,* vol. 15, pp. 4399-4981, 2015.

[47] D. R. Lide, CRC Handbook of Chemistry and Physics, 84th Edition, CRC, 2004.

[48] F. J. Millero, «Thermodynamics of the carbon dioxide system in the oceans,» *Geochimica et Cosmochimica Acta,* vol. 59, n. 4, pp. 661-677, 1995.

[49] A. A. Yawalkar, A. B. Heesink, G. F. Versteeg e V. G. Pangarkar, «Gas–Liquid Mass Transfer Coefficient in Stirred Tank Reactors,» *The Canadian Journal of Chemical Engineering,* vol. 80, n. 5, pp. 840-848, 2002.

[50] G. Chen, M. C. v. Loosdrecht, G. A. Ekama e D. Brdjanovic, Biological Wastewater Treatment: Principles, Modelling and Design, IWA Publishing, 2023.